Faculty of Physics and Astronomy

University of Heidelberg

Diploma thesis

in physics

submitted by

Heiko Hoffmann

born in Schramberg

2000

The dynamics of crack patterns in soil induced by desiccation

This diploma thesis has been carried out by Heiko Hoffmann at the

Institute of Environmental Physics

under the supervision of

Prof. Kurt Roth

Abstract:
Many soil types develop cracks due to desiccation. The resulting crack patterns were simulated with the help of a network of springs, representing the breaking material. A spring breaks if the tensile stress on it exceeds a threshold. Based on existing models in the literature a numerical model was developed. It was used to study the time evolution of cracking and to investigate the final crack pattern. It came out, that the model reproduces some phenomena which can be observed in natural crack patterns (90° angles of intersections, dynamics of emerging cracks). Two parameters of the model - the disorder in the distribution of stress thresholds for the individual springs and a slipping threshold (resembling friction) - were varied and their impact on the crack pattern was studied. It was found that friction induces a characteristic scale. Varying disorder, a continuous transition from loop-like closed cracks (loops) to a system of not interconnected cracks was observed. The number of loops in the topology of the crack pattern, was introduced as an order parameter.
Besides the theoretical part, an experiment was carried out. A bentonite-sand-water mixture was prepared as a layer on a glass plate and dried at room temperature. As a result of drying crack patterns developed. These were recorded by a digital camera. Binary pictures were obtained and the number of loops in the crack patterns of the completely dried mixtures counted. Varying the mass ratio of bentonite to sand a similar transition as in the model was observed.

Zusammenfassung:
Viele Böden bilden beim Austrocknen Risse. Im Rahmen dieser Arbeit wurden die entstehenden Rißmuster mit Hilfe eines Gitters aus Federn, welches das reißende Medium darstellt, simuliert. Eine Feder reißt, wenn die Zugspannung auf dieser einen Grenzwert überschreitet. Basierend auf bestehenden Modellen in der Literatur wurde ein numerisches Modell entwickelt, mit welchem der zeitliche Ablauf des Reißens und das Endstadium des Musters untersucht wurden. Es kam heraus, daß das Modell einige Phänomene reproduziert, die auch in natürlichen Rißmustern auftreten (90° Winkel an Rißkreuzungen, Dynamik der auftauchenden Risse). Zwei Parameter im Modell, die Unordnung in der Verteilung der Zugspannungsgrenzwerte für die einzelnen Federn und die Reibung, wurden variert und deren Auswirkung auf das Rißmuster untersucht. Es wurde herausgefunden, daß die Reibung dem Rißmuster eine charakteristische Größe gibt. Beim Ändern der Unordnung durchlief das Rißmuster einen kontinuierlichen Übergang von ringförmig geschlossenen Rissen (Schleifen) zu einem System aus nicht zusammenhängenden Rissen. Die Anzahl der Schleifen in der Topologie des Rißmusters, wurde als Ordnungsparameter eingeführt.
Neben dem theoretischen Teil wurde ein Experiment durchgeführt. Eine Bentonit-Sand-Wasser Mischung wurde als dünne Schicht auf eine Glasunterlage aufgebracht und bei Raumtemperatur getrocknet. Als Ergebnis des Trocknes entwickelten sich Rißmuster. Diese wurden mit einer digitalen Kamera aufgenommen und in binäre Rißbilder verwandelt. Aus den Bildern der vollständig getrockneten Mischungen wurde die Anzahl der Schleifen ermittelt. Beim Variieren des Bentonit-Sand-Massenverhältnisses wurde ein ähnlicher Übergang wie im Modell gefunden.

Contents

Chapter 1

Overview on cracks

1.1 Motivation

Most studies in soil physics look at soil as a static medium. They take, e.g., a static pore medium and study therein water transport. But, of course, soil is not static and swelling and shrinking due to wetting and drying is one aspect of the dynamics. Understanding the formation of crack patterns as a result of desiccation is one single step towards understanding soil dynamics.
The understanding of crack patterns might be of interest for water transport in soil, which is of interest for contamination of ground water. Large structures like cracks influence greatly the conductivity. The study of desiccation cracks is not restricted to soil. It is, e.g., very desirable to avoid cracks in drying paint.

1.2 Introductory comment

We are dealing with numerical models, experiments and theory. This thesis will be organized the following way. First an overview is given on cracks, especially crack patterns. In the second chapter some approaches to a theoretical understanding of a numerical model to describe cracking will be presented. In chapter three the new numerical model is described. Emphasis is laid on the way friction is implemented into the model. Chapter four presents the results obtained by the model. There, the focus is on the one hand on the dependence of loops in the crack pattern on disorder, and on the other hand on the role of the introduced friction. Chapter five presents an experiment, observing a transition from a polygon pattern to a loop free pattern. The thesis is concluded by a summary of conclusions.

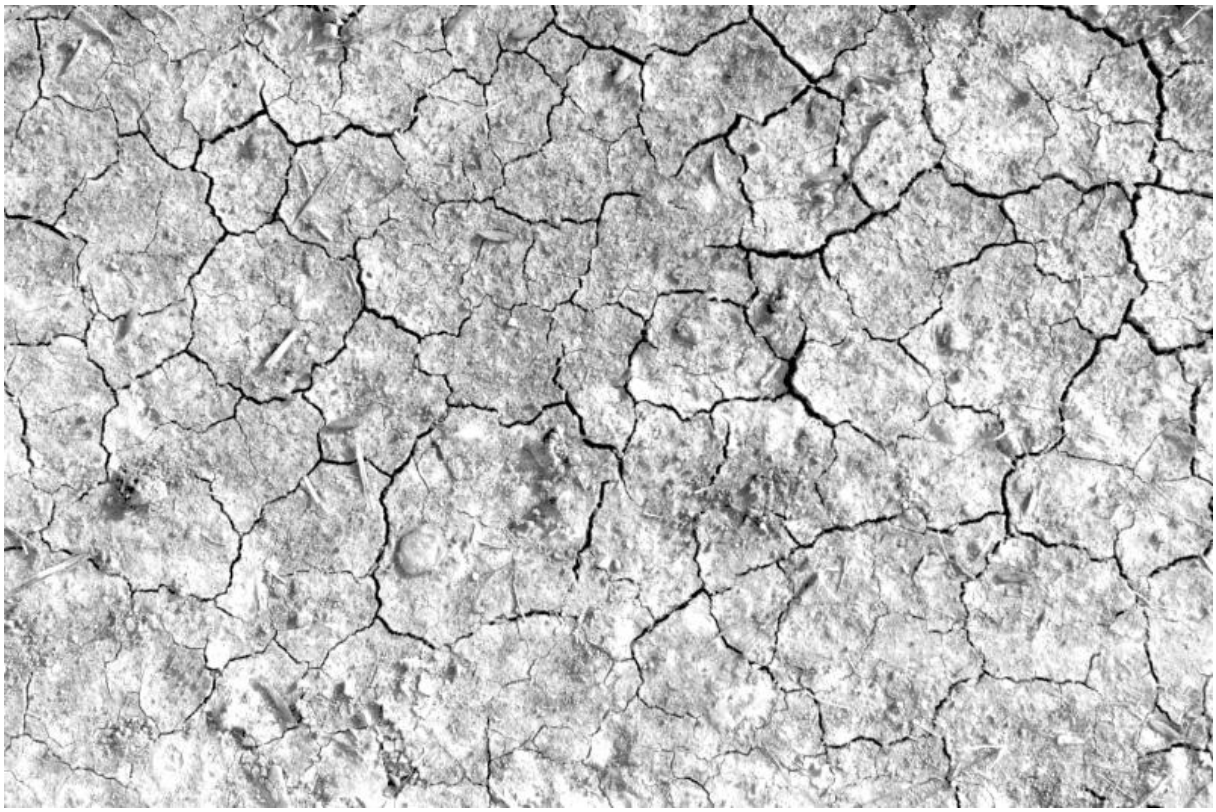

Fig. 1.1: Dry clay rich soil. The width covers about 30 cm.

1.3 Introduction

1.3.1 The importance of cracks in material science

Historically the study of cracks deals with fracture. Ideal materials composed out of a homogeneous lattice of atoms would be by far more stable than real ones [22, 26], i.e. if the failure stress is calculated from the inner atomic forces in such a way that a certain uniform distance - along the direction of the stress - between the atoms is needed for breakage the obtained value is by far (some orders) greater than the one for real materials. The discrepancy can be explained by the presence of defects, tiny cracks, or microcracks [22].
Now, lets look at a crack. Imagine a 2-dimensional cut through a crack. We see an elliptical shape. We try to elongate the material around the crack. The stress at one of the tips of the ellipse is by far greater than the stress on any other point (if a and b are the long and short axes of the ellipse, the stress on the tips is approx. $1 + \frac{2a}{b}$ times the stress at a point far away from the crack [26]). Thus, the material will first break at the tips of an included crack. Describing the material with a discrete lattice or with a continuum field makes no difference to this idea. The material contains defects, e.g. an air bubble. Crack nucleation will start at these bubbles. The stress field is enhanced dramatically near a sharp tip of a crack. This enables breaking of the material due to propagation of the crack.

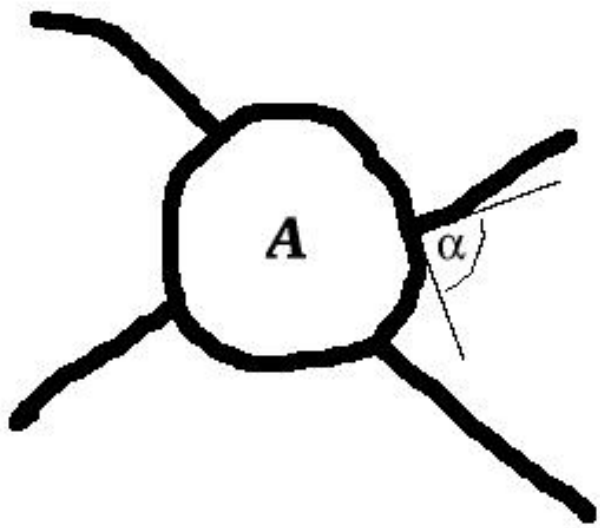

Fig. 1.2: A crack pattern (thick black curve) enclosing of cell (**A**) with a loop. α illustrates what is meant by an intersection angle.

1.3.2 Different fields of study

On the one hand the work done about cracks concentrates on studies of a single crack, especially its propagation. In these studies a plate is put under tensile stress [5]. A crack is initiated by making a small cut into the plate at one side. The velocity of a crack tip rises as a function of the crack length. In heterogeneous materials, interestingly, at some critical value it starts to oscillate, resulting in a lower than expected velocity [5]. Tiny crack branches which develop at the crack tip seem to be connected with this oscillation [28, 27, 11]. In these studies the speed of the crack is very high (above the speed of sound). On the other hand the research efforts deal with the whole network of cracks, with crack patterns. The presented work will focus on the latter one, which attracted only little interest from physics, so far. These patterns can be observed on a wide variety of scales, from cells in dried paint a few millimeters in diameter to giant polygons in deserts several meters wide.
The pattern we will describe are a result of shrinkage which occurs due to the removal of a diffusing quantity (water in the case of desiccation). As the material shrinks internal stresses are built up. The stress is released by cracking. Stresses could be prevented by global shrinking. Therefore, it is often argued [7, 29] that a binding (namely friction) of the visible layer to an underlying substrate is responsible for the local accumulation of stress. A crack pattern forms as multiple cracks grow and interconnect.

1.4 Notations

- **Cell, Fragment, Island:** A part of the material surrounded by a crack (marked as **A** in fig. 1.2), it is a path-component of the material.

- **Loop:** A path-connected part of the crack pattern surrounding one island.
- **Intersection angle:** The angle under which one crack merges with another one (see α in fig. 1.2, the angle between the tangents at the intersection).

1.5 Experiments

1.5.1 Intersection angles

What can we find out experimentally about crack patterns? One might think of the angle of intersection at crack junctions or of the number of sides of the fragments [32].
Both have been studied on a pattern produced by thermal shock in ceramic material [17] and on a shrinkage-crack pattern obtained from an alumina-water mixture after drying [29]. The experiments were all 2-dimensional in the sense that only layers were studied, ceramic disks in one case and mixture distributed on a substrate (a Plexiglas pan) in the other case. The first showed that intersection angles peaked at 120° and the averaged number of sides was between 5 and 6. In contrast the alumina-water slurry gave an angle of 90° ($\pm 5°$) and a maximum for four-sided cells. The desiccation process seems to be somehow different. If the material has enough chance to relax, stresses can build up such that the stress along a crack is much greater that perpendicular to it, resulting in the merging of cracks under 90° angles [32]. The alumina-water slurry is a kind of model experiment to study desiccation, of a similar kind is an experiment on coffee-water mixtures [7]. The latter also showed intersection angles of around 90°.

1.5.2 Island sizes

In the coffee and alumina experiments the influence of layer thickness and bottom friction was also investigated. Greater thickness resulted in bigger cells ($S \propto d^2$, S is the mean cell area and d the thickness of the layer [7, 29]). It was found qualitatively that friction reduces the cell size [7, 29].

1.5.3 Crack speed

The propagation speed of one crack in a desiccation process is by far slower than in the single crack experiment above. Groisman et al.[7] estimated the speed from video recordings. They observed during the desiccation of a coffee-water mixture a value of 0.2 to 10 mm/min.

1.5.4 Fractals

A fractal is a set of points with a metric which is self-similar [2]. This means it is similar on different scales. In the case of fractals in nature the precise mathematical definition of similarity is weakened, and approximately similar is meant by similar.
An interesting experimental setup was performed by Skjeltorp et al.[30]. A monolayer of uniformly sized spheres with a diameter of 3.4 μm was confined between two parallel

glass sheets. The spheres disperse in water. Thus letting the whole thing dry the spheres shrink and stress is built up (between the spheres). Isolated defects grow. Cracks grow very rapidly at the tips. This gives them a linear shape. Later on, when more stress has been released new cracks get more irregular. In the final pattern there is a hierarchy from wide to thin cracks over one order of magnitude. Skjeltorp et al. claim that the resulting crack pattern is a fractal.

1.6 Numerical models

How can we build up a model to produce crack patterns? We make a mesoscopical approach, i.e. we do not make a model on the physical basis of all the atoms involved. This would be useless. It is too complicated and would demand to much computer power. Instead we subdivide our medium into small segments interconnected with springs. We assume that locally the material can be described to first order by a linear stress-strain relation. Strain is the elongation of a material under stress. This assumption fails if we have plasticity. The later means that if stress is removed again the material will not return into its initial state.

1.6.1 Describing a model

We will look at the problem in two dimensions. The first spring lattice of choice is a triangular one (fig. 1.3). A square lattice is less stable. In the latter, if we shift two parallel rows of nodes we obtain zero stress to first order. There is no shear stress. The next-nearest to nearest neighbor distance relation is also in favor of the triangular lattice ($\sqrt{3} > \sqrt{2}$). Therefore ignoring direct next-nearest neighbor interactions is less serious. Most desiccation studies have been performed on triangular lattices [23, 16, 12, 14]. But, also some work was done on square lattices (probably because of simplicity) [19, 10].
For every bond in the lattice one Hookean spring is taken. They are connected with each other at the nodes, around which they are free to rotate.

Now, for every node in the lattice the force on it looks like this:

$$\vec{F_i} = \sum_{j \in N_i} K_{ij} \frac{\vec{x_i} - \vec{x_j}}{|\vec{x_i} - \vec{x_j}|} \left(|\vec{x_i} - \vec{x_j}| - d \right) \tag{1.1}$$

N_i is the set of the 6 neighbors of i. K_{ij} is the spring constant of the spring between node i and j. $\vec{x_i}$ is the position vector of the node i, and d is the equilibrium distance of the springs (relaxed spring length).

It is crucial to assume finite d. Zero relaxed spring length would mean, the system behaves like a blown up air-balloon and breaking overstressed springs would result in a collapse. This is not the way we expect soil to be. But note, finite d makes the equation non-linear. This will mean that we cannot regard this lattice as being a discretization for a continuous linear elastic equation.

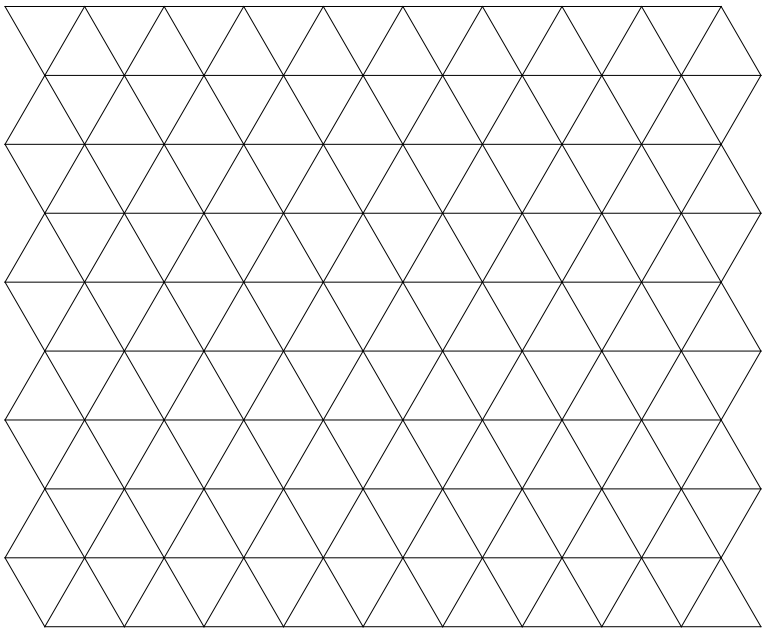

Fig. 1.3: A triangular lattice.

To compute our model we need to do basically two things. Find the equilibrium state for the lattice, i.e. find the values $\vec{x_i}$ which make all forces F_i vanish (relax the lattice). Second, remove a spring (a bond in the lattice) if it exceeds a certain stress threshold T_{ij}. The stress σ_{ij} on a bond between the nodes i and j is $K_{ij}|\vec{x_i} - \vec{x_j}|$. Removing the bond is realized by setting $K_{ij} = 0$. We will only remove springs which are over-stressed and not those which are over-compressed. This is reasonable for wet soil.

This is the basis for most models. In fracture problems typically an external stress is expend on the top and bottom row of the lattice (e.g. [9]). Between two elongation steps the lattice undergoes an algorithm like the one described in fig 1.4. This requires a sufficiently slow elongation.
Now, we do not want to compress or stretch a piece of soil. We put it as a layer on top of a substrate. To study such situations a slight modification of equation (1.1) is used:

$$\vec{F_i} = \sum_{j \in N_i} K_{ij} \frac{\vec{x_i} - \vec{x_j}}{|\vec{x_i} - \vec{x_j}|} \left(|\vec{x_i} - \vec{x_j}| - d\right) + K^0(\vec{x_i} - \vec{x_i^0}) \tag{1.2}$$

Here, we have additional springs which attach the layer to a substrate with a uniform spring constant K^0. The $\vec{x_i^0}$ are firmly attached to the substrate. This kind of model was introduced by Meakin [23]. In comparison he did not use a deterministic rule for breaking springs (as it is described above), but a stochastic one, i.e. there is just a probability for breaking a spring depending on its stress. We will further deal only with the deterministic rule.
Our layer just lives in two dimensions and we look on the top of it. But, a real soil layer

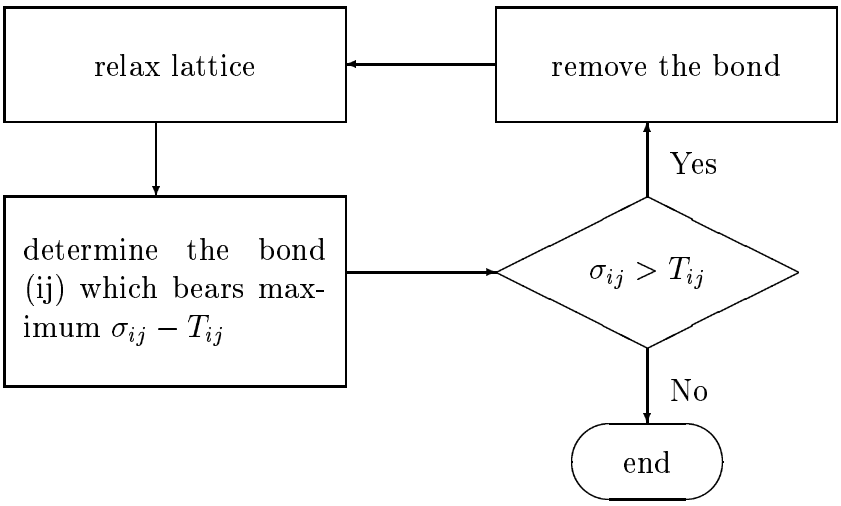

Fig. 1.4: An algorithm to describe cracking. σ_{ij} is the stress on the bond between nodes i and j. T_{ij} the stress threshold.

is of course 3-d. We assume that the crack patterns in a real soil layer are 2-d, in a sense that the cracks percolate rather fast from the top surface to the substrate. This is confirmed by observation, if the layer is sufficiently thin [7]. Therefore, if we would make horizontal cuts through our medium every cross-section would look the same.

How can we impose stress on the system?
Some attempts have been made by lengthening the substrate, in one direction [20] or by lengthening it isotropically in order to simulate desiccation [14]. During the desiccation process water is evaporating making the material shrink and thus increasing the internal stress of the medium. Other attempts to simulate desiccation are to decrease the equilibrium spring length [16, 12].

The material of interest is heterogeneous. How can we implement disorder? We could pick a random distribution for the K_{ij}. In most work the K_{ij} are all equal and the stress thresholds T_{ij} (the set $\{T_{ij}\}$) are randomly distributed (e.g. [14, 20]). As a first choice the distribution might be a Gaussian one (it is the most probable one which maximizes the entropy). It seems to result in crack patterns which are most similar to those in clay [20]. Another preferred distribution is a rectangular one (e.g. used in [14]). There, the range of values can be better controlled.

There is an additional aspect which may be included into the model. The soil layer can slip on the substrate. This can be really observed during cracking (and it is essential to get the 2-d structure as described above). So far our substrate binding springs are firmly attached to the ground. Thus now, we will introduce a second threshold F_s. If the stress on the substrate binding spring is above this threshold, the node on the substrate is moved towards the freely moving node. We introduced friction. This property is realized in the work by Kitsunezaki [16]. There the node on the substrate slips to a position at

which $K_i^0(\vec{x_i} - \vec{x_i^0}) = F_s$ is satisfied.

1.6.2 Alternatives

We mainly presented one type of model. But, one might think of other types, like elastic beams instead of springs [1]. This needs of course more computation. Here the bonds are not free to rotate. But this property is not important for a desiccation process where we have tensile stress and torques can be neglected.
One might introduce dash-pots in line with the springs to implement viscoelasticity (like in the study by Heino et al. [11] which deals with a the propagation of a single crack). But, visible fluidity can not be observed at the time of cracking. Thus we keep to the simple model.
A simpler model was introduced by Colina et al. [4]. Fuses are used instead of springs in the layer. The nodes are attached via resistors to a substrate which consists of parallel lines of increasing voltage. This corresponds to the directional elongation of the substrate in the spring model. Now, instead of positions of nodes we calculate currents at the bonds. Thus, we have a scaler field which is of course easier to handle than a vector field. But, this model is not producing a pattern of connected cracks resembling real ones.

1.6.3 Results

The desiccation models produced crack networks with islands in between [14, 16, 12].
In the desiccation experiments a peak at 90° crack intersection angles could be observed (see section 1.5). Can this be reproduced in a numerical model? No study we know of has attacked this question seriously. One has to be very careful because the geometry of the lattice leads to preferential directions of crack propagation. This can be clearly seen in Meakin's model[23]. However, higher disorder seems to reduce this effect [14].
Hayakawa [10] computed a 3-d cubic lattice including springs connecting next-nearest neighbors. The algorithm based on the one in Fig. 1.3 and on equation (1.1). The dynamic variable was the equilibrium spring length. There were no constraints at the boundaries (thus also no periodic boundary conditions). He studied directional cracking due to an imposed desiccation gradient. The cracks started at the surface. Regular columnar structures were formed as the cracks proceeded downward. The number of sides peaked at 6. The structure is similar to the one found at the Giant's Causeway in Northern Ireland [32], basalt columns forming a regular pattern. Directional cracking (from the surface downwards) is believed to be responsible for the regular structure [32].
What was the result of the introduced friction? The Kitsunezaki model [16] revealed qualitatively that less friction leads to bigger cells. Thus, it matches the experimental results in [7, 29].
Can we say something on dynamics? Hornig et al.[14] evaluated the mean fragment size in dependence of the elongation of the substrate. It came out as a power law and the exponent depends on whether the disorder (in the distribution of T_{ij}) is strong or weak.

1.7 Empirical models

So far, we restricted our search to mesoscopic models. Of course, there exist empirical models of crack networks which ignore the physics underneath it. For example, one work is describing the crack propagation with a random walk [13]. A crack is described by successive steps of lines and random turns. The maximum range of each of these turns had to be set sufficiently small (3° to 11°) to assure that the crack proceeds in some direction. But, a look at fig. 1.1 reveals that very sharp (90°) turns in nature exist. Further, it was assumed that new cracks always start at the boundary of an existing one. This is in contradiction with observations (see section 5.2).

1.8 Criticality

Under certain circumstances (with the right pressure) the transition between water and vapor is continuous. At the transition point (T_c), there happens something interesting. The density $\rho(x)$ (at a local volume) is a fluctuating quantity and it looses a characteristic scale. This scale-invariance happens to be a characteristic phenomena of continuous phase transitions [3].
Is cracking a process of small and big avalanches (the progress of a crack in a time interval)? It is fascinating to think of the possibility of a critical point at which these avalanches become scale invariant.
Leung and Andersen (LA)[19] studied these avalanches in a spring block model. The model is inspired by the earthquake model by Olami, Feder and Christensen (OFC) [24]. In the OFC model blocks arranged on a square lattice and interconnected with springs were put between two plates, one fixed plate and a moving plate. The blocks rest on the fixed one. A block is only moved if the force on it exceeds a threshold T_s. Every block is connected with a spring to the moving plate. The latter moves very slowly increasing the forces on the blocks. If one block exceeds its threshold it is moved to its equilibrium position altering the forces on the other blocks and possibly causing avalanches of block slips (number of slips between two consecutive steps of the moving plate). The model exhibits self-organized criticality (the fluctuations are scale invariant without the need of parameter to match a critical point. The system organizes itself - during the dynamics - towards a critical state [15]).
In the model by LA there is no moving plate. Instead, stress is imposed by increasing the uniform spring constant. A second threshold is introduced, a stress threshold T_c, beyond which a spring breaks. They varied the ratio of the two thresholds $\kappa = T_c/T_s$ and observed a phase transition. The final crack pattern was qualitatively different. For a large value of κ, the cracks were very much interconnected like in a net pattern. The other phase showed localized and non-percolation cracks. At the phase transition they could observe a power law in the probability distribution of the crack avalanches.
But, one has to be careful to compare crack dynamics with self-organized criticality. The system is not dynamically invariant. If a crack occurs it lasts. Islands formed by surrounded broken bonds naturally restrict the size of the events happening in these islands to the size of the island. Thus, this results in an additional finite size effect later

on in the cracking process.

Chapter 2

Theory

The theory chapter will deal with the description of the discrete spring lattice. No continuum mechanics is considered. The purpose of this chapter is to prepare for the ideas of the following chapters.

2.1 A one-dimensional model

Often a problem which is unsolved in 2 dimensions can be easily solved in one dimension, like the percolation problem [31]. Thus, what can we find out about the one-dimensional spring lattice?

Consider a configuration as in fig. 2.1. The springs connected to the substrate are

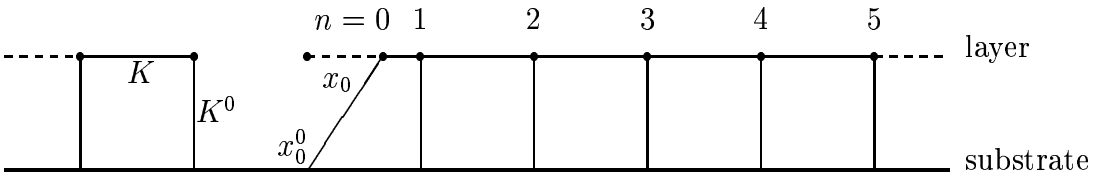

Fig. 2.1: A one-dimensional spring lattice with substrate attachment springs. One bond is removed (a 1d crack). Thin lines represent springs. The vertical elongation of the substrate attachment springs (vertical lines) is zero (here it is not zero for illustration reasons).

firmly attached to it (no friction). Their spring constant is K^0. Let the binding position $x_n^0 = n$. The springs in the layer have the spring constant K. Let x_n be the displacement of the node n (relative to x_n^0). The bond to the left of $n = 0$ is missing (a crack). As a result from this removal, we want to calculate the displacements x_n if the forces are in

equilibrium.
The equilibrium condition yields the following equations:

$$(x_{n+1} - x_n + 1 - d) + (x_{n-1} - x_n - 1 + d) - \frac{K^0}{K} x_n = 0 \tag{2.1}$$

$$(x_1 - x_0 + 1 - d) - \frac{K^0}{K} x_0 = 0 \tag{2.2}$$

We rewrite them and substitute $\kappa = \frac{K^0}{K}$:

$$x_{n+1} - (2 + \kappa)\, x_n + x_{n-1} = 0 \tag{2.3}$$

$$x_1 = (1 + \kappa)\, x_0 + d - 1 \tag{2.4}$$

We assume that the displacement vanishes at infinity. Note, this is only valid if $\kappa \neq 0$. Thus, we will restrict our solution to $\kappa > 0$. Now, we have a further boundary condition:

$$\lim_{n \to \infty} x_n = 0 \tag{2.5}$$

We will solve the equations with the following ansatz: $x_n = a\, \lambda^n$. Substituting this expression for x_n in (2.3) yields:

$$\lambda^2 - (2 + \kappa)\lambda + 1 = 0 \tag{2.6}$$

$$\Rightarrow \lambda_\pm = 1 + \frac{\kappa}{2} \pm \sqrt{\kappa + \frac{\kappa^2}{4}} \tag{2.7}$$

Only λ_- is smaller than 1. Thus, (2.5) cancels λ_+ and our solution looks like $x_n = a\, \lambda_-^n$. Using (2.4) we get a.

$$a\, \lambda_- = (1 + \kappa)\, a + d - 1 \tag{2.8}$$

$$\Rightarrow a = \frac{1 - d}{\frac{\kappa}{2} + \sqrt{\kappa + \frac{\kappa^2}{4}}} \tag{2.9}$$

Thus, our solution is:

$$x_n = \frac{1 - d}{\frac{\kappa}{2} + \sqrt{\kappa + \frac{\kappa^2}{4}}} \left(1 + \frac{\kappa}{2} - \sqrt{\kappa + \frac{\kappa^2}{4}}\right)^n \tag{2.10}$$

$$\Rightarrow x_n \propto \exp(-\frac{n}{\xi}) \tag{2.11}$$

with $\xi = -1/\ln(\lambda_-)$. Our x_n decays exponentially. For simplicity, we look at $\kappa \ll 1$. In this case we have:

$$\xi \approx \frac{1}{\sqrt{\kappa}} \tag{2.12}$$

A very similar derivation can be found for the fuse model in [4]. The 1-d fuse model behaves exactly like the 1d spring model. ξ is called the characteristic length. Its physical meaning is the interaction range of one crack. The larger the value for κ (the strength of the connection to the substrate) the smaller the characteristic length. We can also say the binding to the substrate induces a characteristic length.

How is the stress distributed around the crack? We compute the length l of the bonds:

$$l_n = 1 + x_{n+1} - x_n = 1 + (1-d)\frac{\frac{\kappa}{2} - \sqrt{\kappa + \frac{\kappa^2}{4}}}{\frac{\kappa}{2} + \sqrt{\kappa + \frac{\kappa^2}{4}}}\lambda_-^n \tag{2.13}$$

$$for\ \kappa \ll 1 : l_n \approx 1 - (1-d)\lambda_-^n \tag{2.14}$$

Now, the strain s (the elongation beyond the relaxed length) of a bond is $l_n - d$. With equation (2.14) we get $s = (1-d)(1-\lambda_-^n)$. At infinity the strain is just $1-d$, the initial value. But, close to the removed bond (1d crack) it is smaller (s increases with the distance from the crack). The stress is simply $K\,(l_n - d)$. Thus, the stress is reduced around the crack. Where will a new crack occur? Let the stress threshold be randomly distributed, with a probability density $p(T)$. The probability P_n that the bond between n and $n+1$ breaks is:

$$P_n = \int_0^{K(l_n - d)} p(T)dT \tag{2.15}$$

Around a crack a new crack will occur less likely. In contrast, in the 2-d model the probability is increased at the crack tips. In a 1-d model there are no crack tips. This makes the crack dynamics qualitatively very different. But, a 1-d crack can be regarded as a cross-section of a 2-d crack. At the sides of such a crack the probability for new cracks is reduced.

But, a look at fig. 2.2 reveals that this picture is a bit too simple for the 2-d case. If an elliptical crack is formed all the bonds on its boundary are stretched (the ones at the tips the most). Just the bonds perpendicular to the crack behave like in the 1-d case and shrink. This leads to the following result. One crack approaching the side of another crack will merge most likely in a 90 degree angle. The stress along a crack is much bigger than the perpendicular one. This can be also observed in real mud [32]. We see, this interesting behavior is already included in a spring lattice model.
With the numerical model it can be further observed that at some degree of disorder in the distribution of $\{T_{ij}\}$ the crack boundary is zigzag shaped. This reduces now the probability of new cracking for all bonds around one crack (again things are different at the tip).

2.2 Crack initiation

Now, we will investigate the effect of removing a single bond in a 2-d lattice. Again, we want to calculate the displacements resulting from the removal of one bond. We take a

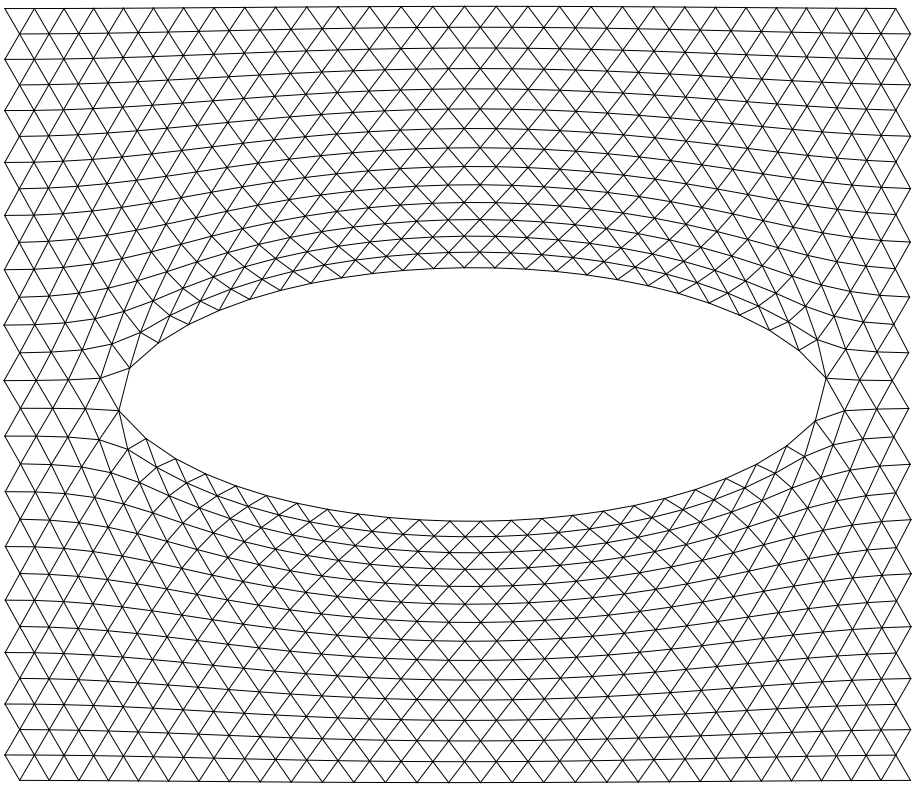

Fig. 2.2: The displacements of the nodes around a crack in the 2-d case. The cracks consist of 45 removed bonds and the lattice has $30 * 30$ nodes. A relaxed spring length $d = 0.7$ is used.

triangular lattice without any bonds attached to a substrate. The unbroken lattice should be fixed, e.g. wrapped around a torus with constant size, such that it can contain elastic energy without being able to contract. As in section 1.6 we will use real springs with a relaxed spring length d. The length of one bond is initially set to 1 (without loss of generality). The spring constant is uniformly 1.
The dashed bond in fig. 2.3 will be removed and we will calculate the amount by which the bonds printed as thick lines are stretched. We make a first approximation. The positions of the nodes 2 to 6 will not be effected by the removal of the bond.
We calculate the energy of the five bonds connected to node 0 and minimize the expression to get the position of node 0. Because of the symmetry there will be no displacement in the y-direction. Thus, the problem stays one dimensional. To calculate the energy we make a further approximation. We develop the square root around d^2 to first order:

$$\sqrt{dx^2 + dy^2} = \sqrt{dx^2 + dy^2 - d^2 + d^2} \approx \frac{1}{2d}(dx^2 + dy^2 - d^2) + d \tag{2.16}$$

This results in the following energy expression (constant factors were omitted):

$$E = \sum_{j=2}^{6} (dx_j^2 + dy_j^2 - d^2)^2 \tag{2.17}$$

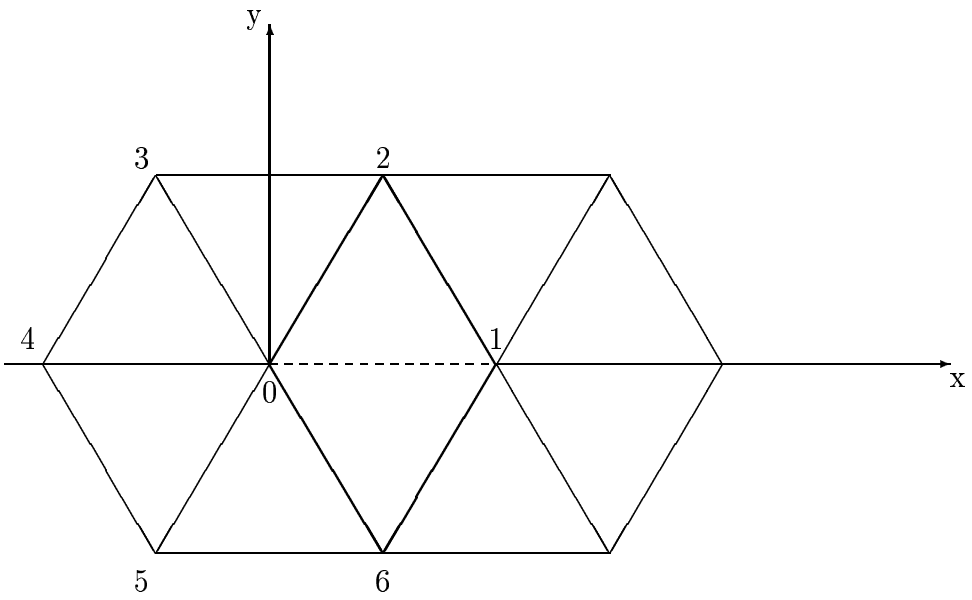

Fig. 2.3: A single bond crack. Illustrated is a part from the triangular lattice. The dashed line is the bond going to be removed. The origin of the coordinate system is the position of node 0 before the removal of the bond.

Now, plug in the positions of nodes 2 to 6.

$$E(x) = ((x+1)^2 - d^2)^2 + 2((\frac{1}{2}+x)^2 + \frac{3}{4} - d^2)^2 + 2((\frac{1}{2}-x)^2 + \frac{3}{4} - d^2)^2 \qquad (2.18)$$

x is the position of node 0. Now, setting $\frac{\partial E}{\partial x} = 0$ we get:

$$5x^3 + 3x^2 + (9 - 5d^2)x + 1 - d^2 = 0 \qquad (2.19)$$

x will be small (of an order smaller than 1). Thus, we neglect the x^3 term, just to keep the expressions simple. For $d = 1$, x must be zero. This cancels the second solution for x. Now, x reads:

$$x = \frac{5d^2 - 9 + \sqrt{(9-5d^2)^2 - 12(1-d^2)}}{6} \qquad (2.20)$$

For $d = 0$ the approximation (2.16) fails. But, in the case of $d = 0$ x can be easily calculated without the approximation: $x = -0.2$. Thus, to get a better result for x as a function of d we will alter the above expression to fit $x = -0.2$ at $d = 0$ by multiplying it with $(1 + a(1-d))$ and choose a appropriately (this will not alter $\frac{\partial x}{\partial d}|_{d=1}$). The result is shown in fig. 2.4.

From this result we get immediately the elongation of the thick bonds. This is shown is fig. 2.5.
Now, again the elongation of a bond is directly connected to the probability of its breakage (equation 2.15). If we describe desiccation we decrease d from 1 to some value > 0.

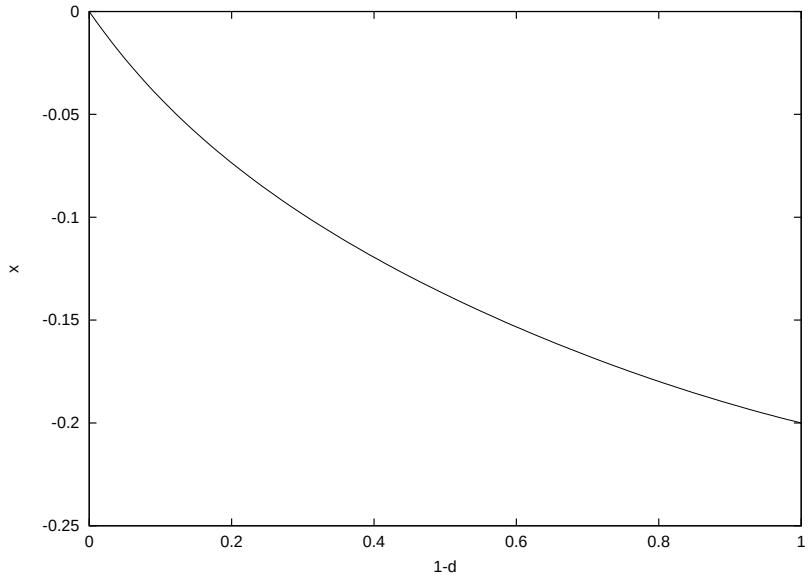

Fig. 2.4: The displacement x of node 0 as a function of $1 - d$ (d: relaxed spring length).

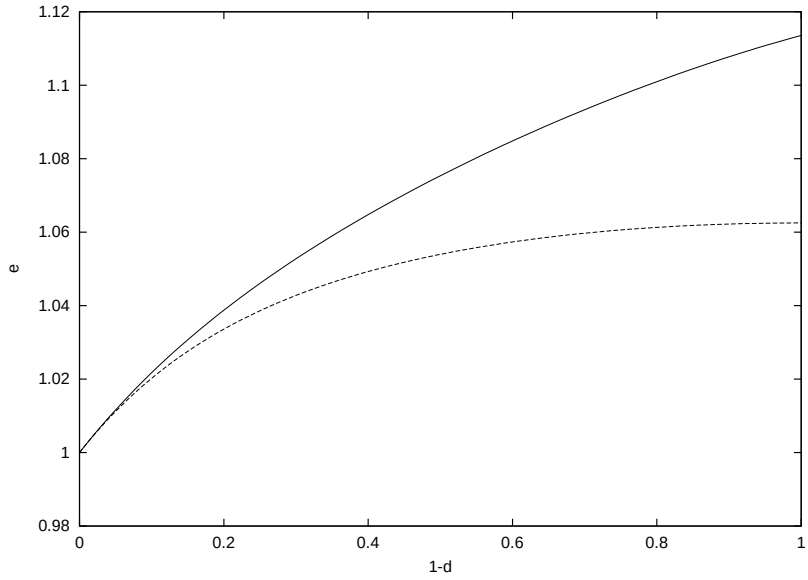

Fig. 2.5: The elongation e of bond (02) as a function of $1 - d$ (d: relaxed spring length). The dashed line shows the result without the correction for $d = 0$.

Comparing the elongation e of a bond at the crack boundary (thick lines) to the elongation of any other bond (there $e = 1$) we see that the difference is rising with decreasing d (see fig. 2.5). Important is the relation of breaking probability at the crack tip to the probability somewhere else in the lattice. Thus, if the breakage of a bond occurs later in time (smaller d) the probability is increased that the crack will further develop.

Chapter 3

Numerical model

3.1 The Basics

A numerical model is developed on the basis of section 1.6. A triangular lattice is used with the shape as in fig. 1.3 identifying opposite sides (periodic boundary conditions). The latter will reduce finite size effects and we don't have to care about nasty things happening at the boundary. The lattice size is L, this means there are L^2 nodes and $3L^2$ bonds. The length dimensions of the whole lattice are fixed during the desiccation, this means that we can think of the lattice as wrapped around a torus which has a fixed size (see fig. 3.1).

We use the same nearest neighbor interaction as in (1.1).

$$\vec{F_i} = \sum_{j \in N_i} K_{ij} \frac{\vec{x_i} - \vec{x_j}}{|\vec{x_i} - \vec{x_j}|} \left(|\vec{x_i} - \vec{x_j}| - d \right) \tag{3.1}$$

No substrate attachment springs will be used. K_{ij} is set equal to zero for broken bonds and 1 otherwise (this is no loss of generality, since we are only interested in the equilibrium position, respectively in $F/\frac{\partial F}{\partial x}$). The initial distance to the next neighbor bond is

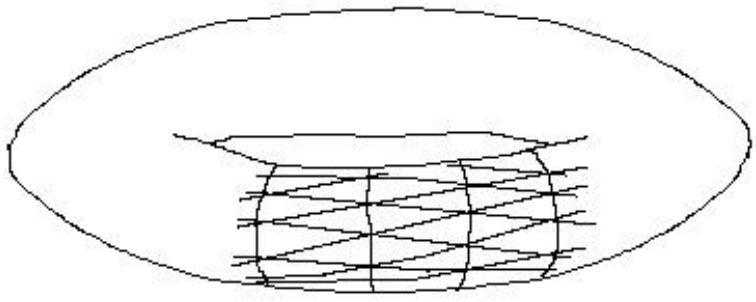

Fig. 3.1: The triangular lattice with periodic boundary conditions can be visualized as wrapped around a torus.

set equal to 1 (again this value is of no meaning). The desiccation is simulated by slowly decreasing d starting from 1 and going down to some value d_{min} (we can equivalently think of letting d fixed and blow up the torus). d_{min} will be set to a value of the order 1 (we used 0.65). The length of a bond will not differ much from d. Therefore, we develop the square root in (3.1) around d^2 to first order as in (2.16). Thus, the energy for node i as a function of its neighbors is:

$$E_i = \sum_{j \in N_i} K_{ij}(|\vec{x_i} - \vec{x_j}|^2 - d^2)^2 \tag{3.2}$$

Again universal constants are omitted. This correction proved to be of no influence to the resulting crack patterns, but of great increase in calculation speed.

Disorder was introduced with the choice of thresholds T_{ij}. Each T_{ij} is given independently a random value. The random values were Gaussian distributed, centered around T_0 with a standard deviation σ. Taking a rectangular distribution many bonds become suddenly critical when the relaxed spring length d reaches $1 - T_{min}$. This does not seem to be a realistic description of nature. A cut-off was implemented in the Gaussian distribution to avoid negative values. If a T value gave a negative result a new random value was chosen. The random numbers were taken form the random number generator called 'ran2' from the Numerical Recipes by Press et al [25].
Equivalently the T_{ij} could have been set to a fixed value and the K_{ij} could have been assigned random values. This showed to be of no difference to the result. The only difference is that we cannot expect same results for the same standard deviation of the Gaussian distribution. The deviations in the K_{ij} compensate some amount of the standard deviation (bonds with high K move together closer, this reduces the probability of breakage). K_{ij} was chosen to be fixed because it's easier to handle theoretically (as the reader might have recognized in the discussion before).
Initially the positions of the nodes were not put exactly to their equilibrium position. Every coordinate was altered with a random value from -0.1 to 0.1. The desiccation process starts with the relaxation of the lattice. Thus, altering the initial positions around their equilibrium positions does not make a significant difference. Actually, it did not influence the results. All motions of nodes in the model basis on their positions the time step before. The prevention of too much regularity at the starting point motivated the described randomness.
Fig. 3.2 shows the algorithm for the desiccation process. For every run new distributions $\{T_{ij}\}$ and $\{x_i\}$ were chosen. As can be seen in fig. 3.2 after every removal of one bond the lattice is relaxed completely. Only if no more bond breaks d is decreased further. This means the desiccation is infinitely slower than the breaking process. Between two bond removals the lattice has infinitely many time to relax.
The desiccation step δ is of no importance as long as it is small enough. We do not need to carefully decrease d by an infinitesimal amount to assure that only one bond breaks at once because the lattice is relaxed after every bond removal.

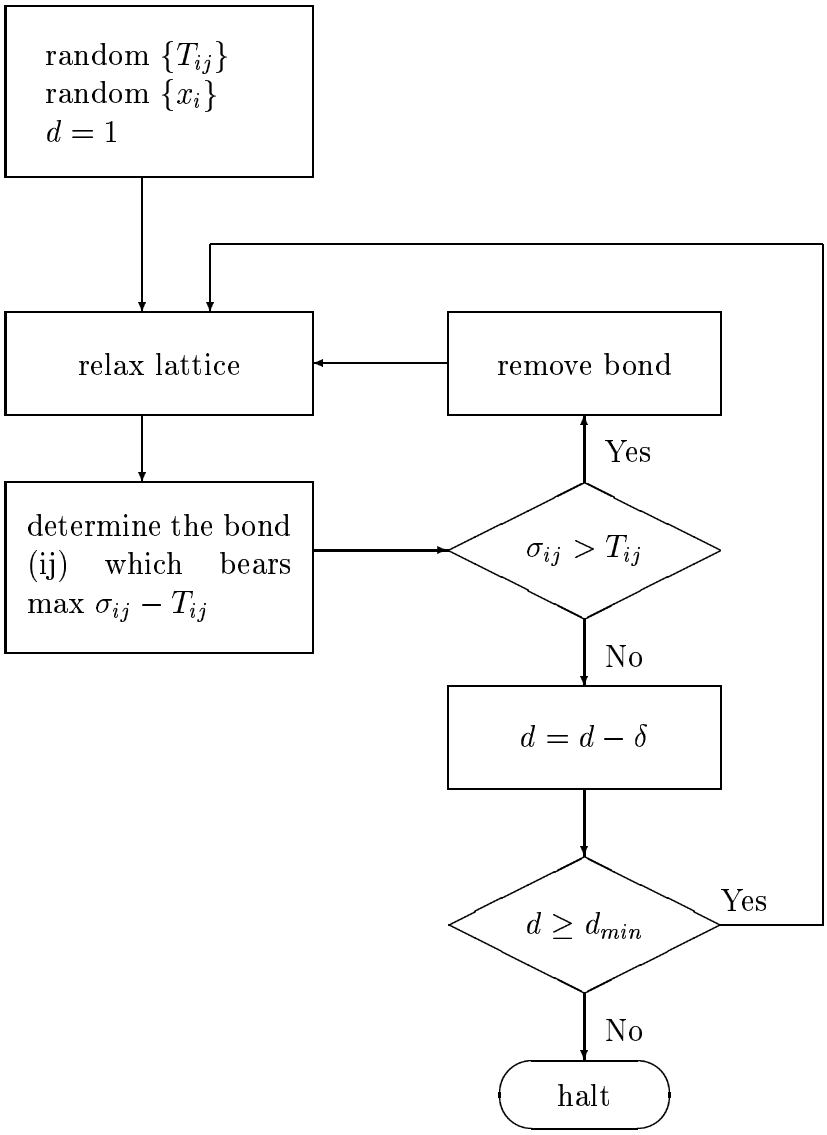

Fig. 3.2: The algorithm to describe desiccation. d is the relaxed spring length. σ_{ij} is the stress on the bond between nodes i and j. T_{ij} the stress threshold.

3.2 The relaxation

3.2.1 Iterative process

An iterative relaxation was used. It works like a cellular automaton (e.g. [6]). That means, there is a discrete lattice, every point in it has the same predefined neighborhood and its values at the time $t + 1$ are a function of the values of its neighborhood points at the time t.
In one time step every single node is relaxed for itself as a function of the positions of the nodes in its neighborhood. The node is moved towards its equilibrium position. This is

realized with the Newton-Raphson method [18], a Newton iteration for many dimensions (here two). To move the node from the position $\vec{x_i}$ closer to the position of the minimum of the function $E_i(\vec{x_i})$ a paraboloid is fitted to $E_i(\vec{x_i})$ at $\vec{x_i}$ and the position $\vec{x'_i}$ of its minimum is determined:

$$\vec{x'_i} = \vec{x_i} - H_E^{-1} \nabla E|_{\vec{x_i}} \tag{3.3}$$

For the energy E expression (3.2) is used. H_E is the Hesse-matrix of $E_i(\vec{x_i})$. If the change in position $|\vec{x'_i} - \vec{x_i}|$ is larger than a critical threshold ϵ, x is set to x' and the whole iteration step is repeated until the change in position is less than ϵ. Fig. 3.3 illustrates the relaxation algorithm.

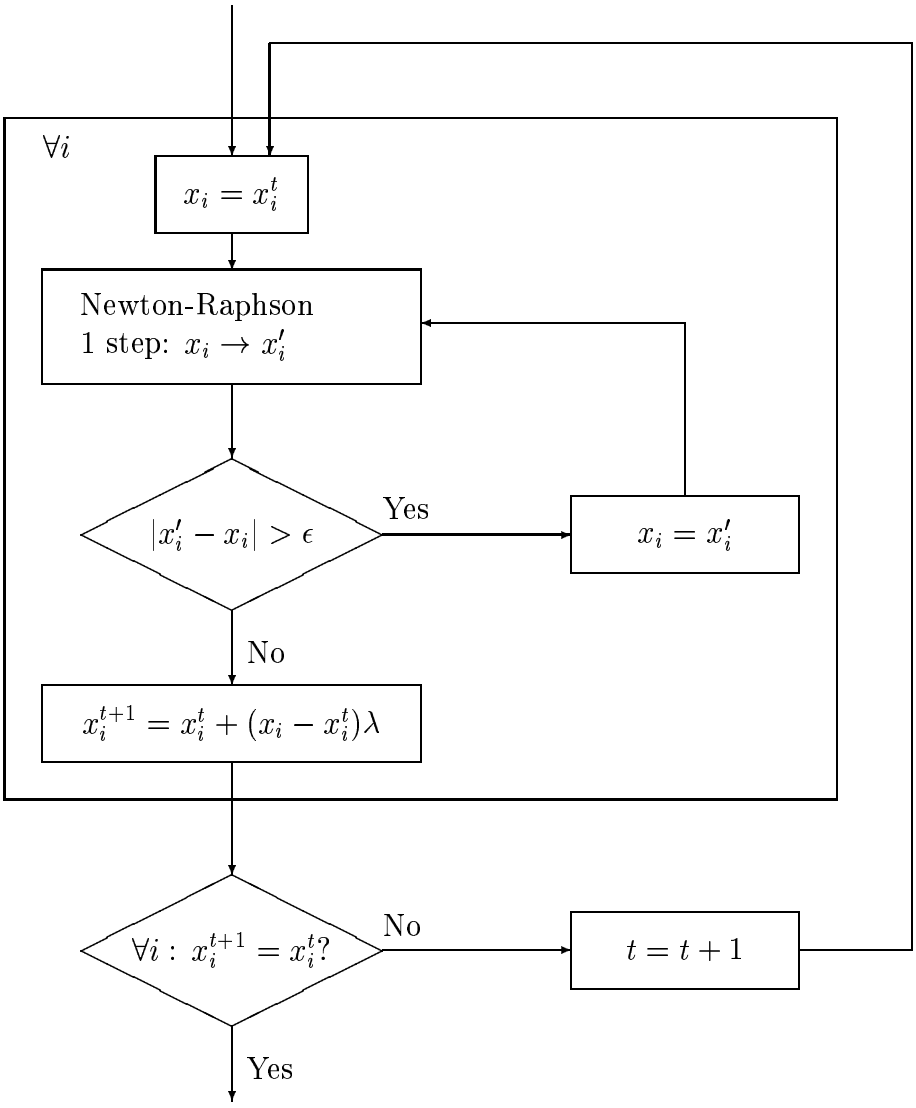

Fig. 3.3: The relaxation process. All x variables are 2-d vectors.

3.2.2 Explanation of the parameters

What is our ϵ doing? It is not only a necessary constant for stopping the iteration, but it has also a physical meaning. ϵ is a threshold for slipping. It is a kind of friction. Before a node is moved a quantity has to exceed a threshold. Here it is the force divided by its derivation. Seems strange, but doing this we can keep everything in the units of the initial length of a bond. It will be easier to see the impact of ϵ on the model (see section 3.5). It is intuitive that the slipping threshold results in the relaxation dying out at some distance from a distortion. A big ϵ gives the lattice less chance to relax between the breaking of two bonds. We will see that it induces a characteristic length scale. But, in contrast to the model of Meakin [23] the nodes can slip on the substrate and it is realized without the use of additional springs (in contrast to the work by Kitsunezaki [16]). This is a new approach for models controlling the desiccation with the relaxed spring length. The motivation of introducing slips was, that it enables cracks to increase their width during the desiccation process. Thus, cracks developing later will be thinner. This hierarchy can be observed in nature (see fig. 5.7). Besides the role of ϵ to describe friction, we suggest that it can also model some inner properties of the material (without any substrate), like plasticity. The slipping threshold prevents the material to behave ideally elastic.
As can be seen in fig. 3.3, we introduced a further parameter, λ. What is its meaning? It was introduced for numerical reasons. It has been found that in some rare situations oscillations can occur in the lattice, such that the condition $\forall i\, x_i^{t+1} = x_i^t$ is never fulfilled. This is very nasty. But, with a choice of $\lambda < 1$ these effects could be reduced. However, it has a small impact on the cracking process. Reducing λ showed to have of a similar effect on the crack pattern as increasing ϵ (structures get smaller and more peninsulas vs. islands appear). So far, the impact is not well understood. Some discussion can be found in section 3.5. $\lambda > 1$ results in instability. Additionally, a maximum number of relaxation time steps (from t to $t+1$) was introduced to insure the simulation to end. It was set to four times the lattice size L.
To make the numerical procedure more transparent the C source code of the relaxation algorithm is put into appendix A.

3.3 Limitations of the model

The model is just two dimensional. Thus following phenomena can naturally not be considered.

- The vertical cross section of a newly formed crack in clay shows a V-shape. Desiccation starts at the surface, thus the top layer shrinks earlier than the bottom layer.
- Islands of clay bend in the vertical direction.
- Especially in thick layers the impact of the crack surface on the desiccation is important. Water in the soil can only escape via the surface. Thus, there the soil will dry out sooner. The soil shrinks further at a crack surface and new cracks might preferentially start there.

With this model one might study non-uniform shrinking, e.g., the relaxed spring length d is reduced at a crack surface. Or with an appropriate distribution of the d value directional drying could be studied. But, these things are not part of this study.

3.4 Critique of the model

a) Periodic boundary conditions

During a desiccation process a real soil layer (e.g. as prepared on a glass sheet) could shrink as a whole. In contrast this is not possible in the model. The lattice is wrapped around a torus and will not shrink before it breaks. The escape from this problem is that something in the real layer and in the lattice localizes the action. This can be friction and it will induce a characteristic length. Now, the size of the lattice and the real layer need to be much larger than the characteristic length. Otherwise the soil layer just shrinks without any cracks and the torus will break catastrophically leaving a lattice with a boundary behind.

b) The energy has many local minima

We must emphasize that in our model not every bond is under stress. The following situation might be possible. The distance between two next neighbor nodes is smaller than $2d$ and the node in the middle is only connected to these two nodes (all other bonds are already broken), as illustrated in fig. 3.4.

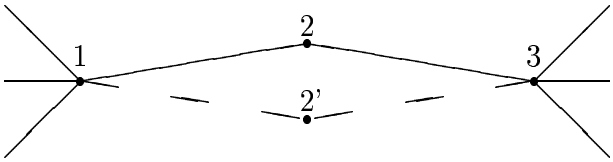

Fig. 3.4: A configuration with two energy minima: 2 and 2'. The length of the bonds (12) and (23) is d, and the distance between 1 and 3 is smaller than $2d$.

Node 2 has two stable positions. This example shows that H_E is not always positive definite. If the node is placed in between 2 and 2' (before the relaxation took place) its energy (according to equation 3.2) has a local maximum. In between this maximum and a minimum there exists a point where H_E gets singular (det $H_E = 0$). This is a problem for the described relaxation of one node. With the above relaxation algorithm node 2 is likely to stay in one of its energy minima. But, big structures bounded between only two nodes like 1 and 3 have been found which oscillate (but, it is very rare). Because of the rareness of these problems they were accepted.

3.5 The role of friction

We will investigate how the slipping threshold ϵ induces a length scale. For simplicity we will set $\lambda = 1$ and let all nodes relax completely to their equilibrium position. We take a one dimensional lattice, remove one bond and look at the equilibrium configuration after the following relaxation. We want to obtain the displacement of a node as a function of its distant from the removed bond, as we did in section (2.1) for the spring attachment model. The initial length of a bond is l.

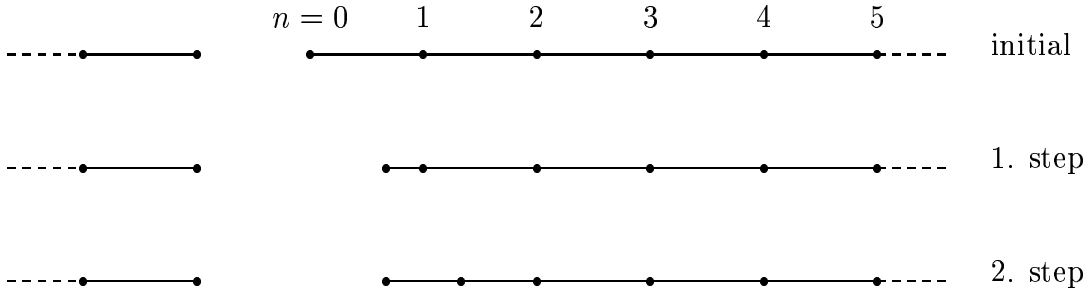

Fig. 3.5: The first relaxation steps in a one-dimensional spring lattice, after one bond was removed.

Let x_n be the displacement of node n. To keep expressions simple we set $l - d$ equal 1. Before the bond breaks all x_n are zero. In the first relaxation step x_0 is set to 1. At every relaxation step the displacement of every node is updated according to the following rule: $x_n := (x_{n-1} + x_{n+1})/2 \ \forall n > 1$ and $x_0 := 1 + x_1$ (the equilibrium position in the context of the neighborhood positions). An update is only performed if the following condition is fulfilled: $(x_{n-1} + x_{n+1})/2 - x_n \geq \epsilon$ if $n > 1$, $1 + x_1 - x_0 \geq \epsilon$ else. The relaxation is stopped if no further displacement is possible. The relaxation here is exactly the same as the relaxation in the one-dimensional variant of the OFC earthquake model [24]. First, the problem is solved numerically. The result for $\epsilon = 0.01$ is shown in fig. 3.6.

Now, we want to study how the characteristic length ξ depends on ϵ. We define the characteristic length to be the intersection of the tangent at $n = 0$ with the n-axes. This way we get the same definition as for the exponential function in section 2.1 (the intersection of the tangent with the x-axes is the point where the value of the exponential function is $1/e$). Trivially the slope of our tangent is -1, and thus $\xi = x_0$. Let n_{max} be the last bond which is affected by the relaxation. It turns out that n_{max} is proportional to x_0. Therefore, we could have also used this value for the characteristic length.

For sufficiently large ξ we find:

$$\xi \propto \epsilon^{-1} \tag{3.4}$$

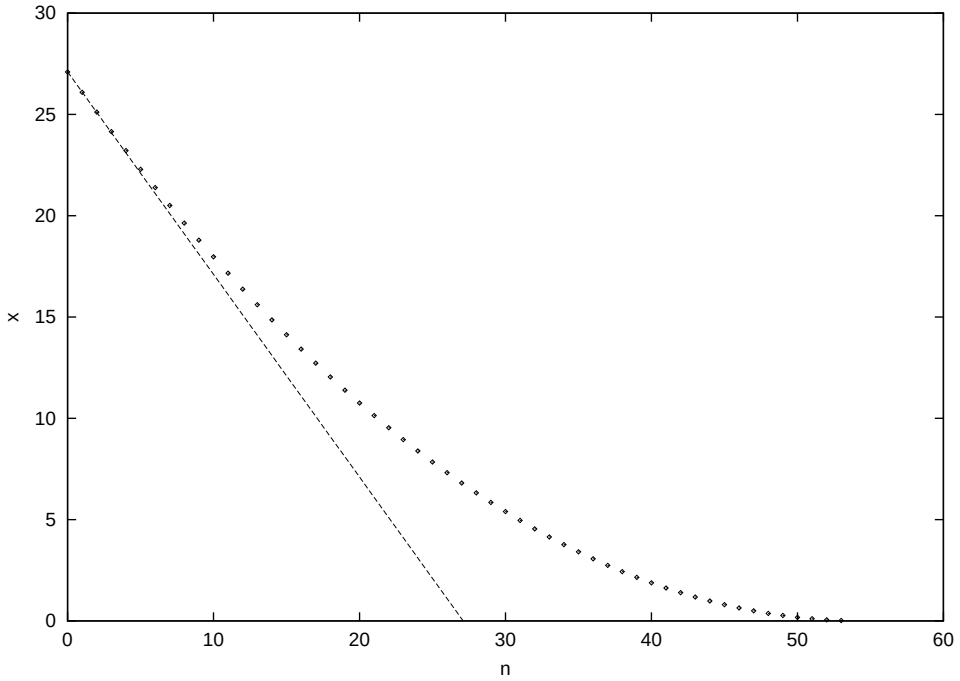

Fig. 3.6: The displacement x of the nodes as a function of the distance ($n = \#\text{nodes}$) to the crack, using $\epsilon = 0.01$. The dashed line is the tangent through $n = 0$.

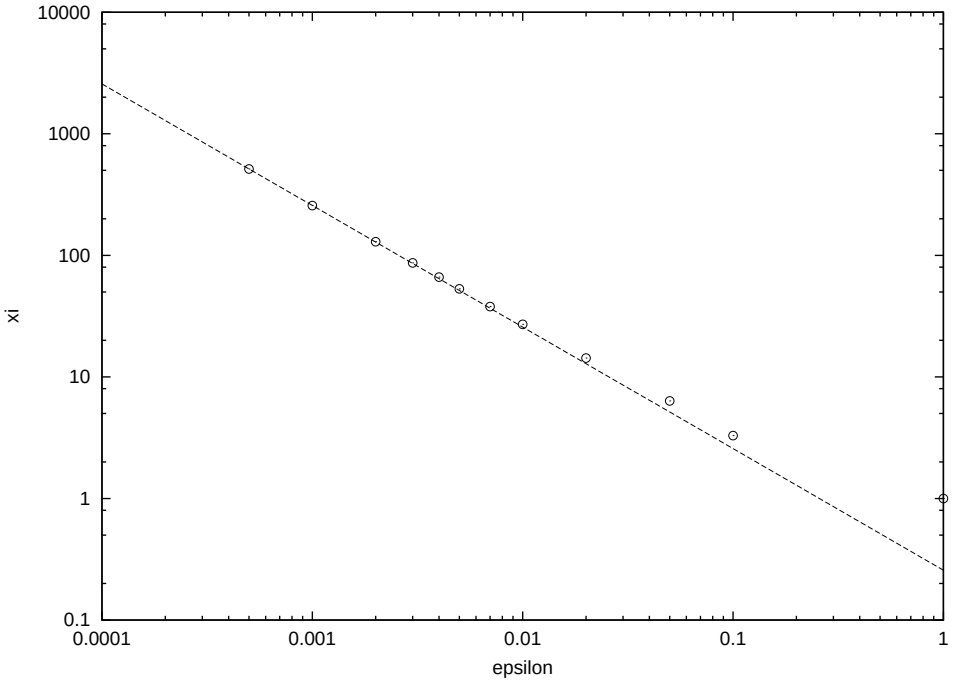

Fig. 3.7: The dependence of the characteristic length ξ (number of nodes) on ϵ. The slope of the line is 1.

It is also not hard to derive this relation analytically. We assume that in the equi-

librium state every node is placed such that it's just at the threshold to jump, i.e. $(x_{n-1} + x_{n+1})/2 - x_n = \epsilon$. Now, the second derivative of any discrete function x_n is $x_{n-1} - 2x_n + x_{n+1}$. Thus, we can readily state $x_n = \epsilon(n_{max} - n)^2$ (a good approximation if the discretization has many points). From this we get $n_{max} = \frac{1}{2\epsilon}$ and $x_0 = \frac{1}{4\epsilon}$.
Introducing $\lambda < 1$ will not change the condition for slipping. We just alter the width of each step, namely $x_n := ((x_{n-1} + x_{n+1})/2 - x_n)\lambda + x_n$. But, this has no impact on the above argument (every node is placed on the edge of the slipping threshold). The numerical solution of the displacement problem supported this thinking. λ showed to be of a minor influence on the characteristic length. For $\lambda = 0.6$ it was reduced by about 2%.

If we turn back to the unit $l - d$ of our model, we get:

$$\xi \propto (l - d)\epsilon^{-1} \tag{3.5}$$

If the displacements are multiplied by a constant $l - d$ same results are obtained if ϵ is substituted by $\frac{\epsilon}{l-d}$.
We expect the lengths in our desiccation patterns to scale like the characteristic length, e.g., cell sizes like ϵ^{-2}.

3.6 Crack cluster

3.6.1 What is a crack cluster in a triangular lattice?

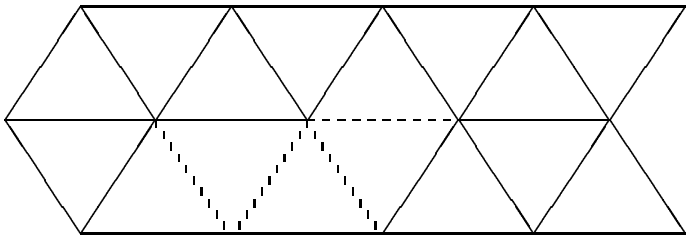

Fig. 3.8: Dashed lines indicate broken bonds. A crack cluster consists of triangles connected by broken bonds.

Fig. 3.8 illustrates what is meant by a cluster. Two triangles connected by a broken (removed) bond belong to one cluster. The size of a cluster is the number of its broken bonds. This is fine because the number of broken bonds is about the total length of a crack. The length of a crack is again connected to its area by a power-law [20, 21]. This way the data can be compared with experiment.

3.6.2 Counting loops

How do we count loops in the crack pattern in our lattice? If the lattice is infinite or has periodic boundary conditions, following relation holds:

$$L = C + b - f \tag{3.6}$$

L is the number of loops, C the number of crack clusters (path-components), b the number of broken bonds, and f is the number of triangles belonging to a crack cluster (i.e. bounded by at least one broken bond).
Let's look at the example in fig. 3.8. Here, $C = 1$, $b = 4$, $f = 5$, and $L = 0$. Equation (3.6) can be proved be induction. For $b = 0$, everything is zero and the equation holds. Assume the equation holds for a given configuration of removed bonds. Now, one more bond will be removed ($b \to b + 1$). We have to consider the following situations:

1. The bond is in between two triangles not belonging to a crack cluster (non-crack-triangles)
   $\Longrightarrow f \to f + 2$, $C \to C + 1$, $L \to L$
   (A new crack cluster emerges, the number of loops stays the same.)

2. The bond is in between a crack-triangle and a non-crack-triangle
   $\Longrightarrow f \to f + 1$, $C \to C$, $L \to L$
   (One crack cluster grows, the number of loops is not changing.)

3. The bond is in between two crack-triangles

   (a) the two triangles belong to different clusters
   $\Longrightarrow f \to f$, $C \to C - 1$, $L \to L$
   (Two clusters merge, no loop appears.)

   (b) the two triangles belong to the same cluster
   $\Longrightarrow f \to f$, $C \to C$, $L \to L + 1$
   (A loop is formed. This way, a single node, a node without any bonds attached to it, will be counted as a loop. But, single nodes can never occur in our model.)

The equation holds thus for $b + 1$ broken bonds. The induction is complete.

3.6.3 Percolation

We define what we mean by a crack cluster percolating the lattice. Assume that x, y are the coordinates describing the torus. A crack cluster is said to percolate the system if it contains either every x coordinate or every y coordinate.

Chapter 4

Results

First we look at some examples to get a feeling how things happen. For all results in this chapter the model as presented in chapter 3 and the parameters $\lambda = 0.6$, $\delta = 0.0001$, and a mean breaking threshold of $T_0 = 0.3$ were used.

4.1 Crack propagation

A lattice of size $L = 50$ was prepared in such a way that 60 bonds were removed in one line (these removed bonds form not a straight line, but a zigzag one). Then, the whole lattice was relaxed (with the algorithm in section 3.2, $\epsilon = 0.01$ was chosen). The result is shown in fig. 4.1.

To observe how this crack evolves, bonds were removed if thresholds were exceeded

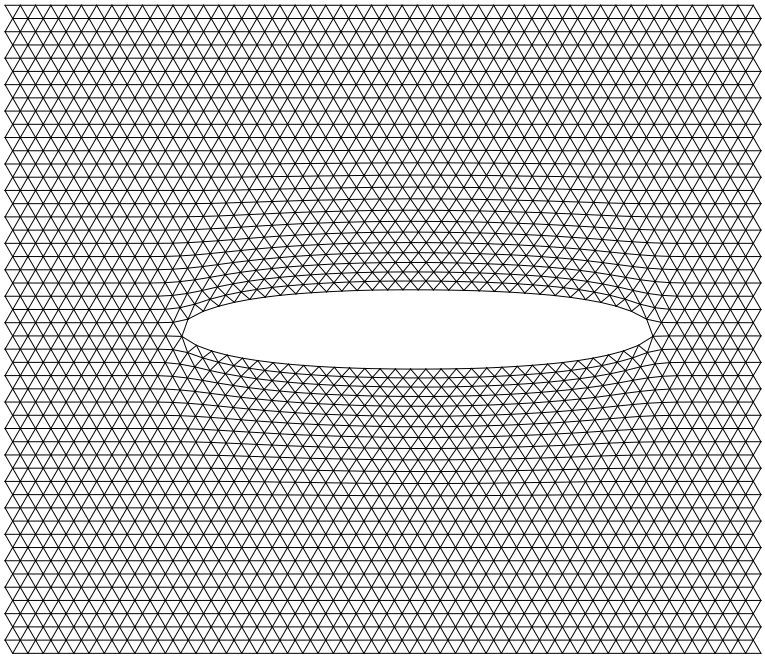

Fig. 4.1: A prepared crack consisting of 60 broken bonds in a lattice with $L = 50$. The lattice was relaxed using $\epsilon = 0.01$.

and the lattice was relaxed after every bond removal (this was perform with a standard deviation of breaking thresholds of $\sigma = 0.09$). After 20 bonds additional were removed the procedure is stopped, and the result can be viewed in fig. 4.2.

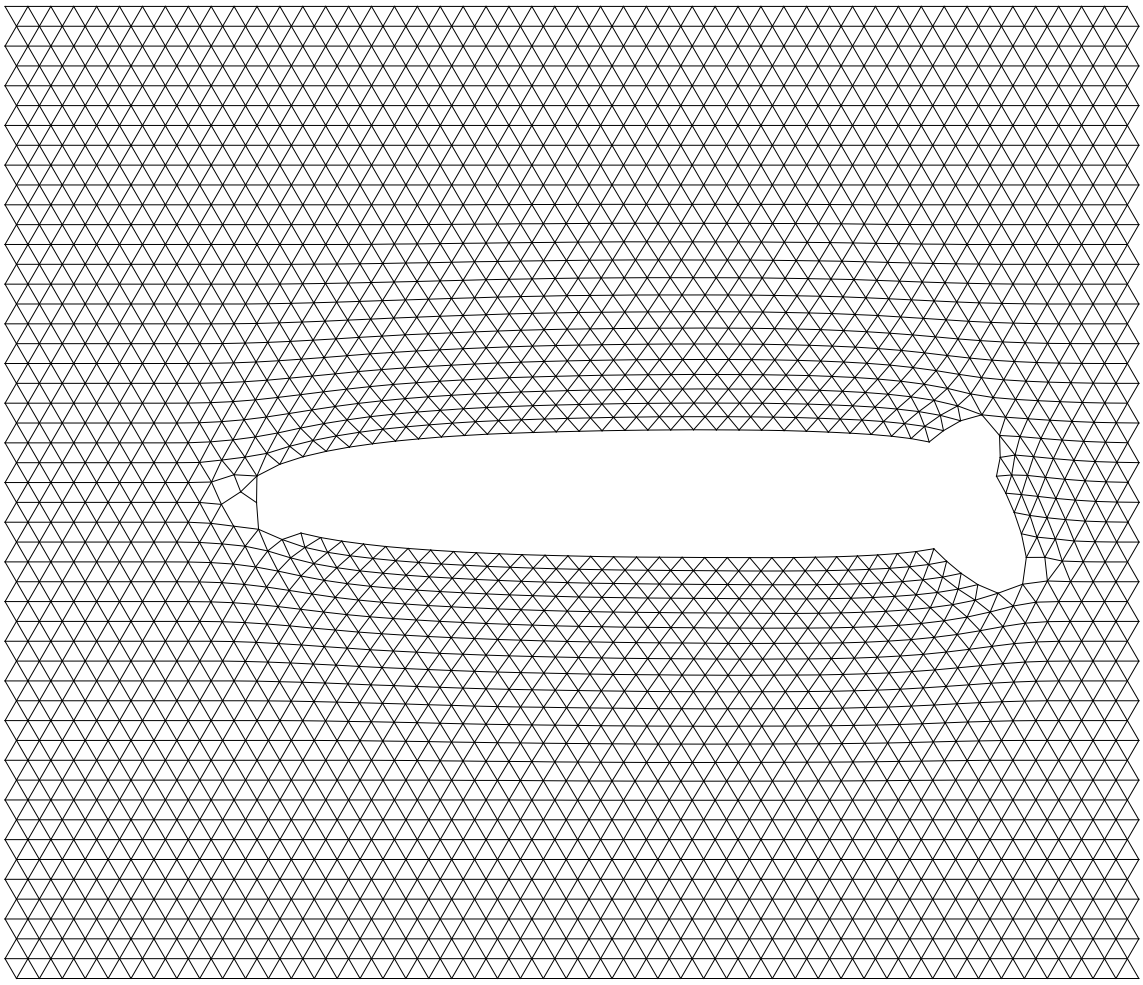

Fig. 4.2: The same crack as in fig. 4.1 after 20 additional bonds were removed.

Now, we will focus on the area around the left crack tip. Microcracks occur in advance of the tip. Stresses are increased in the area around the tip. Because of the randomly distributed threshold not only the bond which bears the greatest stress breaks. Thus, new cracks can occur 'outside' the crack tip. We see our model includes something which is called the process zone. It has been found for clay rich soil that the failure stress of a probe is decreased if the tips of two cracks in the probe are separated by only a short distance around the size of the process zone [8]. The two cracks interact with each other. Probably microcracks form in between.

4.2 The evolution of a crack pattern

We want to observe how the crack pattern develops during the desiccation process. First, we start with an example to illustrate what is happening. We chose a lattice of size $L = 200$, a standard deviation for the Gaussian distribution of breaking thresholds of $\sigma = 0.03$, and $\epsilon = 0.01$ and observe the crack pattern while we decrease the relaxed spring length d. Fig. 4.3 shows the evolution of the crack pattern. Triangles surrounded by three unbroken bonds were colored white.

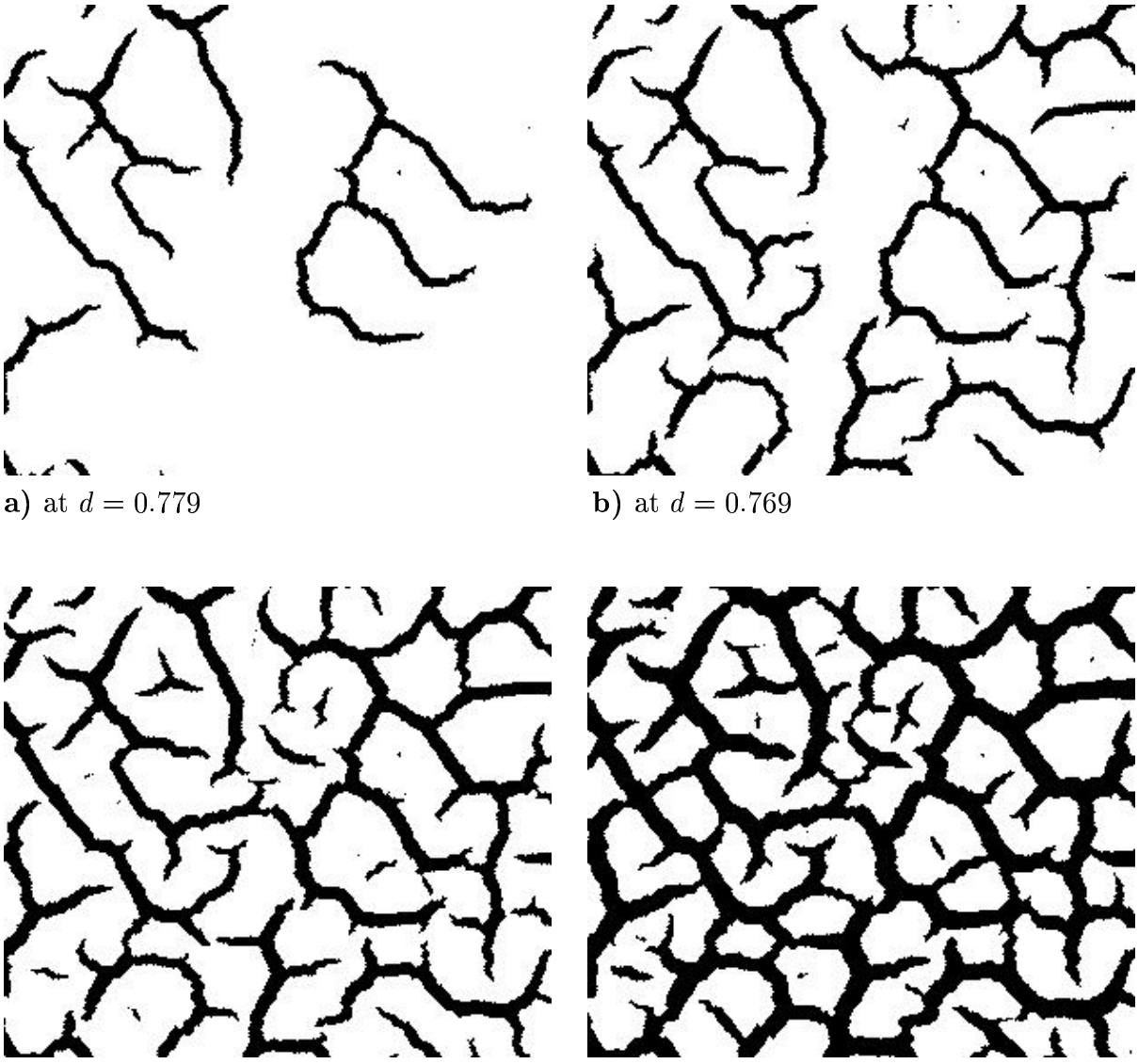

a) at $d = 0.779$ **b)** at $d = 0.769$

c) at $d = 0.740$ **d)** at $d = 0.664$

Fig. 4.3: The pictures show how the crack pattern changes with time using $L = 200$, $\epsilon = 0.01$, and $\sigma = 0.03$. Cracks are colored black.

The pattern looks natural (compare with fig. 5.7). Of course, the pattern depends very much on the random distributions $\{T_{ij}\}$. But, in the context of the parameters above the

shown results are very typical.
We observe that many not path-connected structures were formed. With the ongoing desiccation new cracks emerge, and they emerge in the middle of the white areas rather than on the boundary of an existing crack (this behavior was explained in section 2.1). Loops were formed at about the same time a crack cluster percolates the whole lattice (which is a surprising result). This can be viewed in table 4.1. It shows the d-values for first time percolation (d_P) and first appearance of a loop (d_L) for different lattice sizes L.

	L=100	L=200	L = 300
d_P	0.773 ± 0.011	0.774 ± 0.006	0.770 ± 0.007
d_L	0.764 ± 0.018	0.763 ± 0.012	0.775 ± 0.005

Table 4.1: The d-values for percolation (d_P) and loop creation (d_L). $\epsilon = 0.01$, and $\sigma = 0.03$ were chosen. The results were averaged over 10 (L=100) and 5 (L=200,300) runs.

For other values of σ the difference between d_P and d_L was not significant either. This behavior is not trivial. One might expect that with increasing lattice size loops show up earlier than percolation, because of the localization of the relaxation. But, the 'experimental' finding proves this to be wrong. A crucial point seems to be the merging of two cracks which is not very probable, rather new cracks appear (as can be seen in fig. 4.3). The lattice is covered with cracks before they merge to from loops or a percolating cluster. But, I have no quantitative explanation for this.

Fig. 4.4 shows the dynamics of some quantities for a sample run using the parameters above. In the beginning the energy in the springs rises as $(1-d)^2$ (as expected), but nothing else happens. Then the spring lattice breaks down and the energy is released due to bond removal and shrinkage. In this dynamic phase the number of broken bonds and crack clusters rises dramatically, basically shaping the resulting crack picture. Later on cracks merge forming more and more loops. The number of crack clusters seems to be very high. But, most clusters only consist of one broken bond (these tiny cracks are not shown in fig. 4.3).
It seems to be surprising that the number of crack clusters is not decreasing after loops have formed and clusters have merged to form a large lattice spanning cluster. The explanation is that the total number of crack clusters is dominated by the tiny cracks which still form and compensate the disappearing of clusters. The mass of tiny cracks in a spring lattice model can be also seen in [20] (they used substrate attachment springs).

4.3 The role of disorder

We want to study how the pattern changes if we vary the standard deviation σ of the stress thresholds T_{ij}.

Again, we chose $\epsilon = 0.01$. The relaxed spring length d was decreased until the value $d_{min} = 0.65$ was reached. This d_{min} value was used because at that point most of the

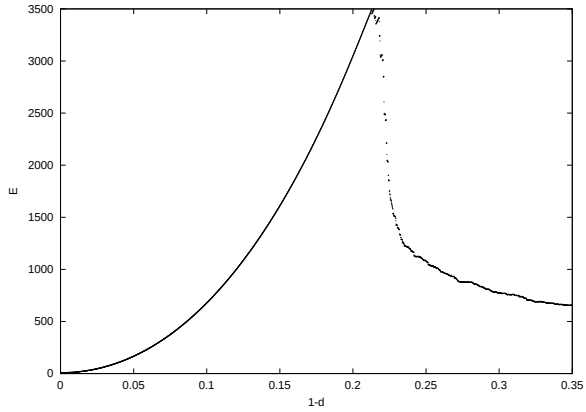

a) elastic energy

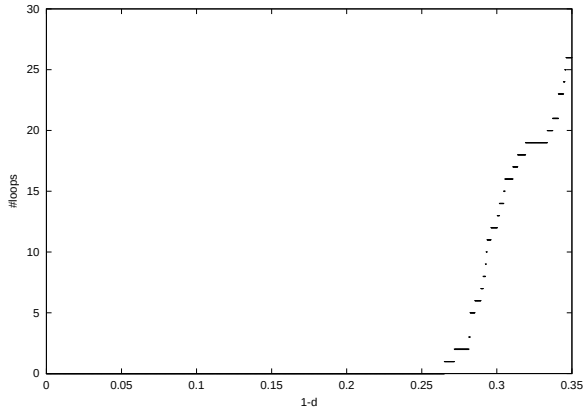

b) number of loops

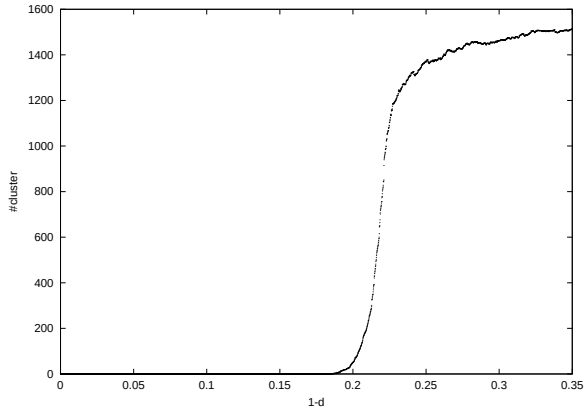

c) number of clusters

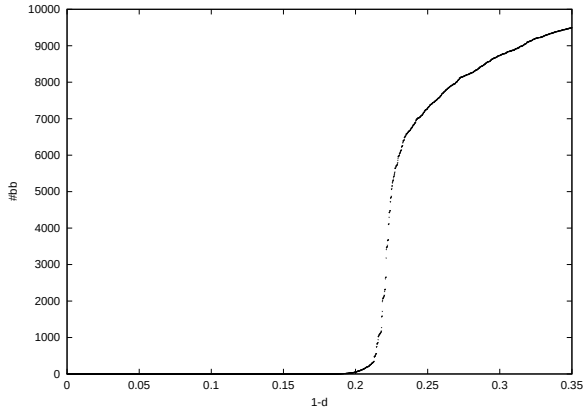

d) number of broken bonds

Fig. 4.4: The dependence of some quantities on $1 - d$ (evolution in time). All values were obtained from one single run with $L = 200$, $\epsilon = 0.01$, and $\sigma = 0.03$.

dynamics has happened. As can be seen in fig. 4.4, the energy and the number of clusters stay about constant. Fig. 4.5 shows typical results for the various σ values.
In fig. 4.5a the symmetry of the underlying triangular lattice induces preferential directions of crack growth (an artifact). Higher disorder cancels this effect. The low disorder case resembles the crack patterns in clay. There, cracks are linear and islands are convex polygons [7]. A similar behavior is found if the slipping threshold is decreased (see section 4.5). If the disorder is increased the crack pattern becomes more and more disconnected. Loops in the pattern vanish. A transition can be observed from convex islands, via peninsulas, to disconnected crack clusters. The patterns can be separated in distinct phases. One phase has loops and a percolating crack cluster, the other one no loops and no percolation. Fig. 4.6 to 4.8 shows how the number of loops at $d_{min} = 0.65$ depends on σ. Before reaching a zero value the number of loops decreases linearly with rising σ. I have no explanation for this linearity (and I do not know if this phenomena has ever been observed before).

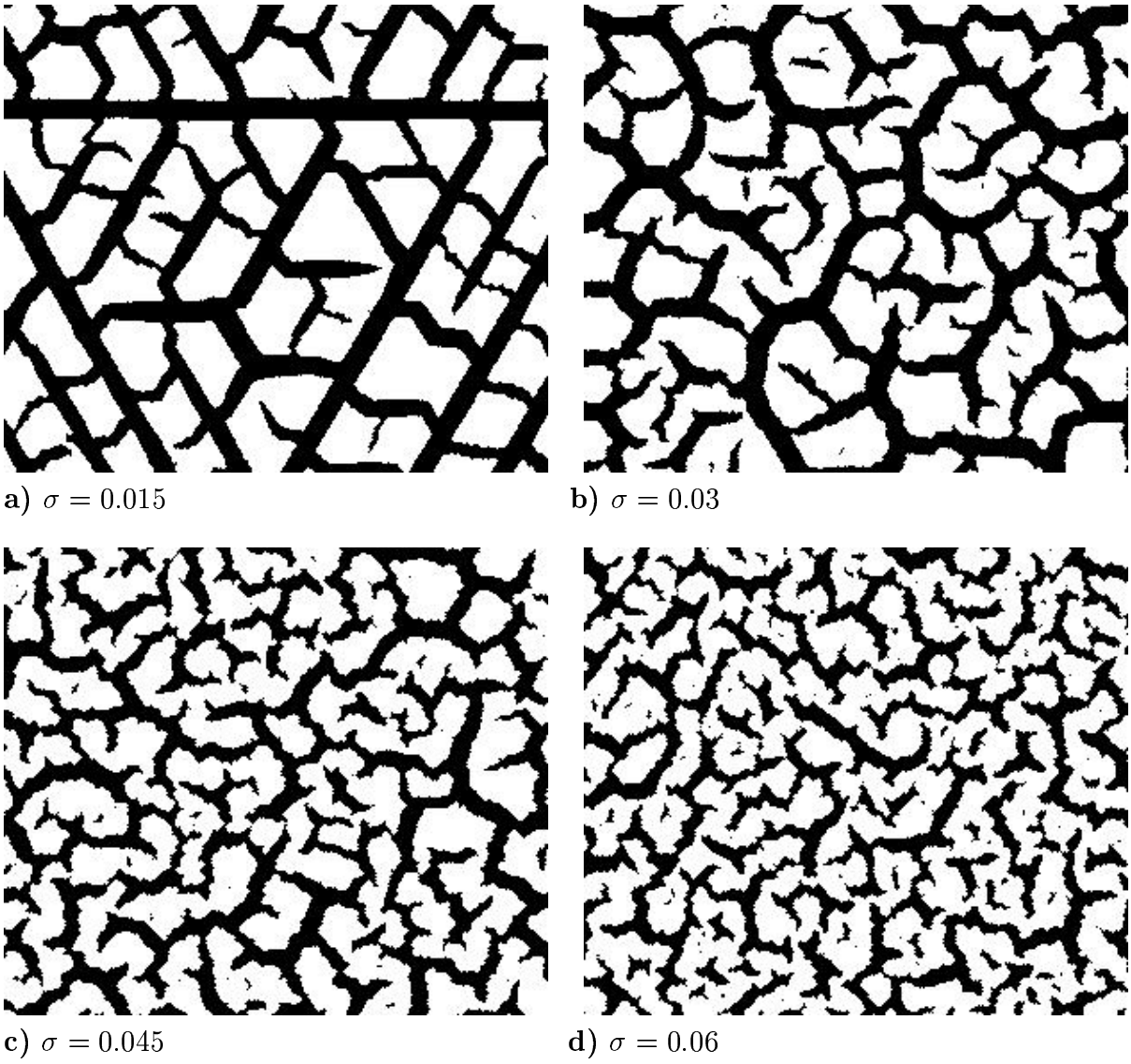

a) $\sigma = 0.015$ **b)** $\sigma = 0.03$

c) $\sigma = 0.045$ **d)** $\sigma = 0.06$

Fig. 4.5: The pictures show how σ alters the shape of a crack pattern, using $d_{min} = 0.65$ and $\epsilon = 0.01$. Pictures were taken after d_{min} was reached.

Lines were fitted to the points on the left side with loop numbers larger than zero (see fig. 4.6 to 4.8). The intersections (called σ_c) of theses lines with the σ-axes are plotted in table 4.2.

L	σ_c
100	0.066 ± 0.005
200	0.063 ± 0.005
300	0.062 ± 0.001

Table 4.2: σ_c (the σ-value above which the number of loops vanish) for various lattice sizes L. Errors were obtained from the linear fit as shown in fig. 4.6 to 4.8

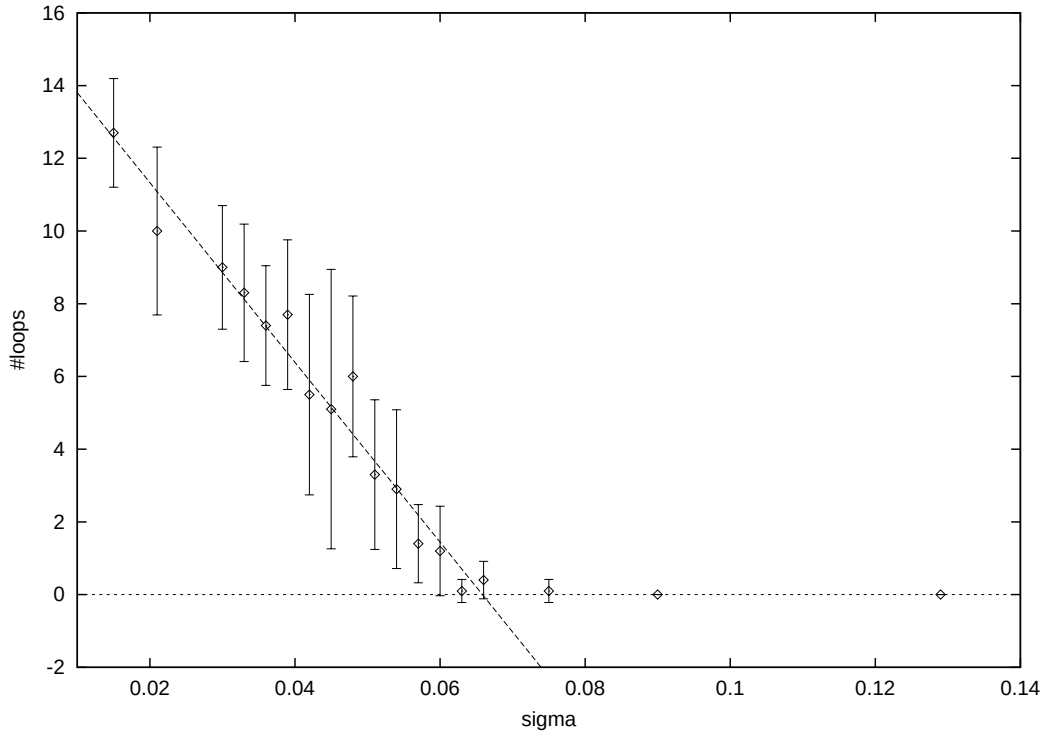

Fig. 4.6: The number of loops as a function of σ, averaged over 10 runs, for $L = 100$. The error bars represent the standard deviations. The dashed line is fitted to the left part of the data (all points, but the three on the right).

The value for σ_c stays in the boundary of the error the same for all investigated lattice sizes ($L = 100, 200, 300$). We conclude that σ_c is an interesting value, and we did not tap into the trap of a finite size effect.
But, the meaning of σ_c should not be overestimated. As can be seen in fig. 4.4d the number of loops depends much on d_{min}. The starting point (d_L) for loop development is also depending on σ (see table 4.3). Using a different d_{min} will shift the whole thing, resulting in a different σ_c.

σ	d_L
0.015	0.760 ± 0.002
0.03	0.763 ± 0.012
0.045	0.717 ± 0.017

Table 4.3: The dependence of d_L on σ, for L=200, $\epsilon = 0.01$, averaged over 5 trials. The standard deviation is systematically increasing for higher σ values.

The number of crack clusters depends less on d_{min} if the value is sufficiently small (as can be seen in fig. 4.4c). In fig. 4.9 the dependence of this number (at $d_{min} = 0.65$) on σ is shown. The number of clusters rise with increasing σ.

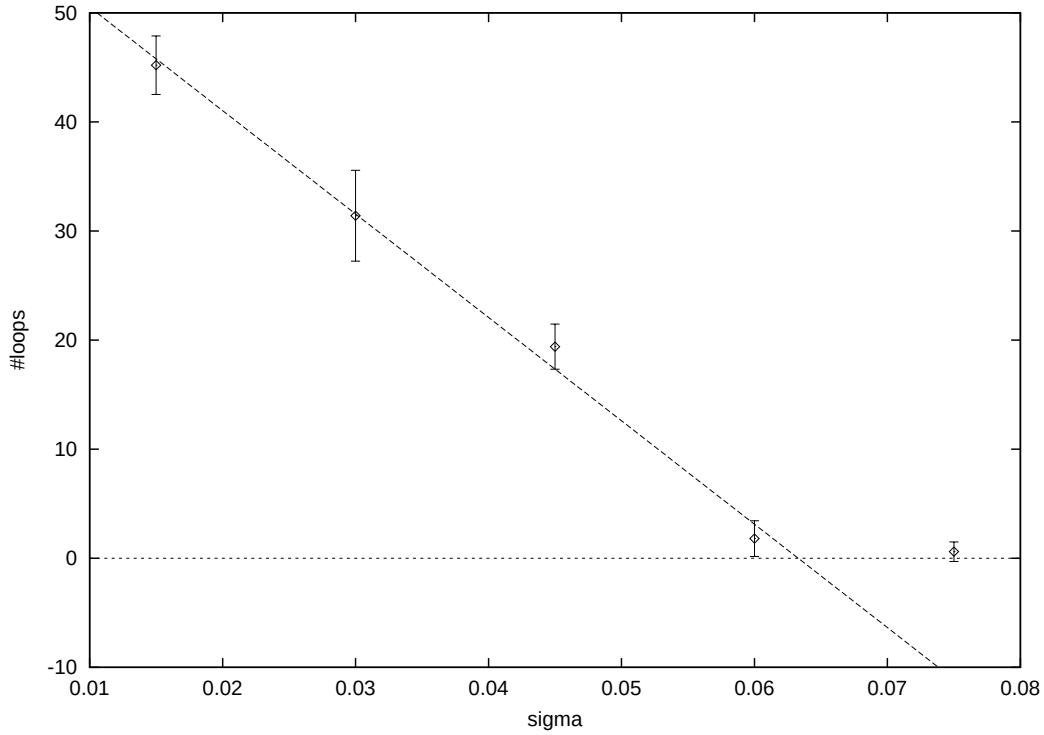

Fig. 4.7: The number of loops as a function of σ, averaged over 5 runs, for $L = 200$. The error bars represent the standard deviations. The dashed line is fitted to the left part of the data (all points, but the one on the right). More data for higher σ-values (as in fig. 4.6) were not obtained due to limited calculation time.

Fig. 4.4 shows that with decreasing d the elastic energy passes a maximum. This maximum value is also evaluated for various σ (see fig. 4.10). Higher disorder reduces the amount of energy which can build up before the lattice breaks down. The maximum decreases with rising σ, as expected.

4.4 Explanation of the dependence on disorder

a) low disorder

It takes a long time until something happens. We must increase $1 - d$ close to T_0. But then, if something breaks the effect of relaxation is much greater (the lattice can contract further with smaller d). The probability that bonds at the crack tips will break is high. Long cracks will develop which percolate the lattice and merge to loops.

b) high disorder

Pretty soon bonds break. But, at that time the probability that they develop further is small (see section 2.2). When a small d is reached, which would allow great relaxation, already many crack clusters have emerged which reduce the lengths l of the bonds (and

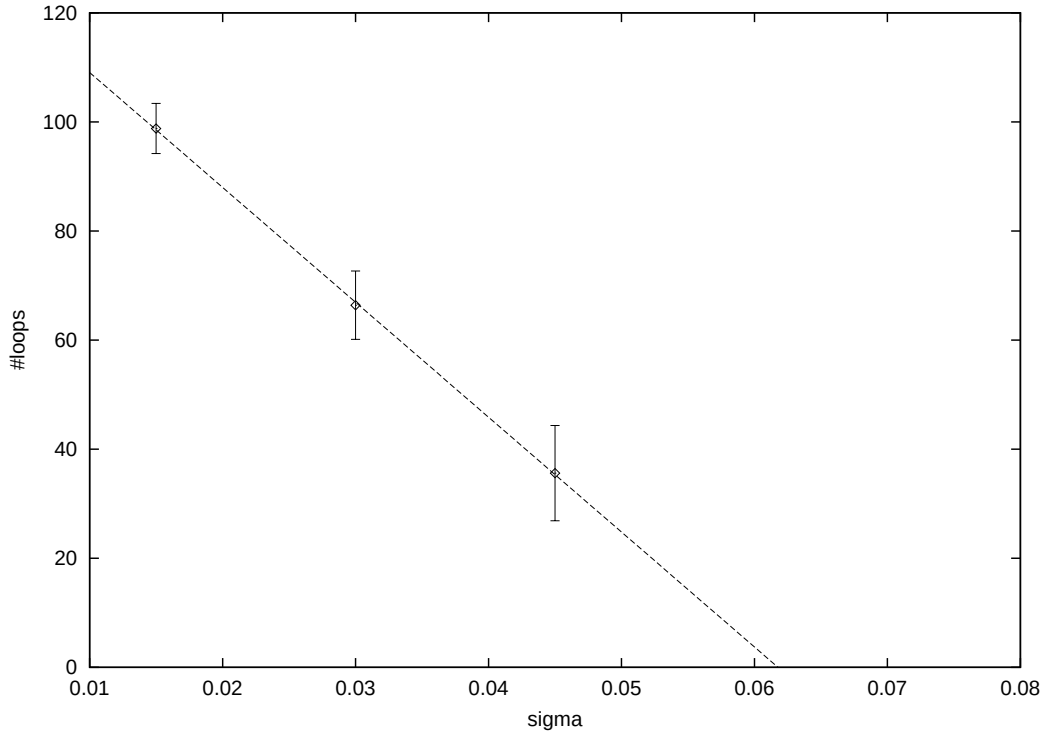

Fig. 4.8: The number of loops as a function of σ, averaged over 5 runs, for $L = 300$. The error bars represent the standard deviations. The dashed line is a fit to the three data points. More data for higher σ-values (as in fig. 4.6) were not obtained due to limited calculation time.

therefore also the elastic energy in the system). With reduced length l we get less relaxation, see equation (3.5). Thus the probability that cracks propagate is reduced. It is less likely that a crack percolates the system. But, why should they not form loops? There are more bonds which can bear a lot of stress and are unlikely to break (especially if no high stresses at crack tips can be produced). If there are sufficiently many of these bonds they form a rigid network which holds together the whole lattice.

To illustrate the idea of breaking probabilities at crack tips as a function of d beyond section 2.2 a crack was prepared in a lattice of size $L = 50$ like in section 4.1. Then d was decreased, the lattice relaxed, and $max_{ij}\{|\vec{x_i} - \vec{x_j}|\}$ (the length of the bond at the crack tip) was plotted as a function of d . Fig. 4.11 shows the result for two different ϵ values $\epsilon = 0.001$, and $\epsilon = 0.01$. The probability of crack propagation rises with decreasing d and with increasing crack length.

The figures also show the impact of ϵ. Higher ϵ also reduces the probability of crack propagation. Thus, we have to expect similar results in the crack pattern for large ϵ as for high disorder (this can be seen in section 4.5). The values for $\epsilon = 0.001$ in fig. 4.11a match pretty good (the $e - 1$ value deviates by -5%) the dashed line in fig. 2.5 (the correction need not be considered, because we always used the altered energy expression). We see, that the approximations in section 2.2 were quite good.

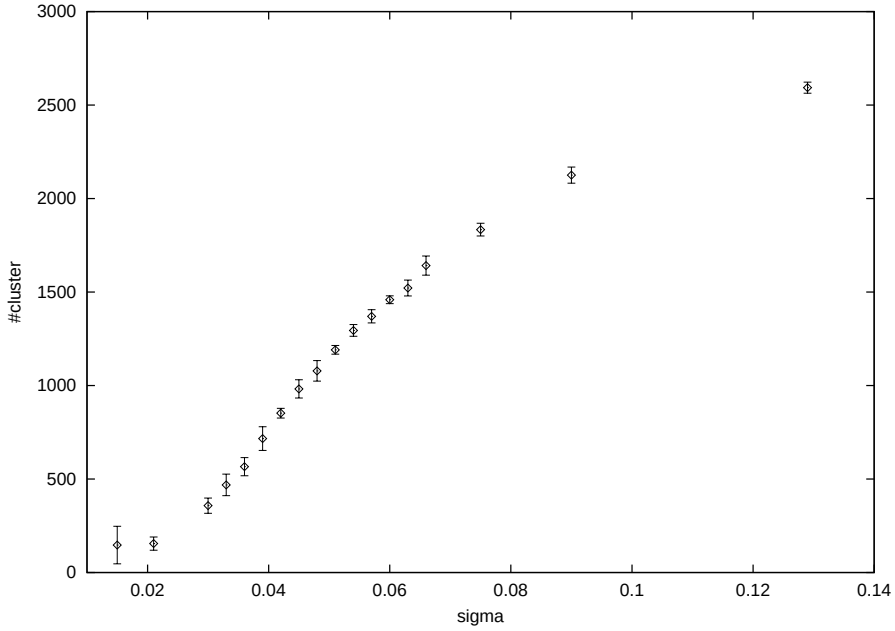

Fig. 4.9: The number of clusters as a function of the disorder parameter σ, averaged over 10 runs. A lattice of size of $L = 100$ and $\epsilon = 0.01$ were used. Error bars represent standard deviations.

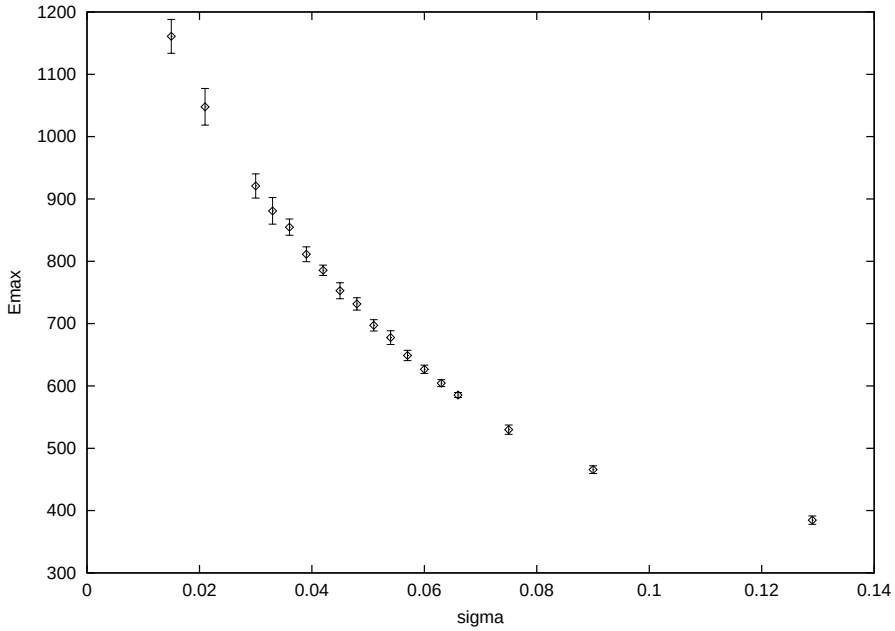

Fig. 4.10: The maximum of the elastic energy as a function of the disorder parameter σ, averaged over 10 runs. A lattice of size of $L = 100$ and $\epsilon = 0.01$ were used. Error bars represent standard deviations. The function is neither a power-law nor exponential.

To check our ideas we compare the evolution of the elastic energy (as in fig. 4.4a) for two different σ values (fig. 4.12). $L = 200$ and $\epsilon = 0.01$ were used.

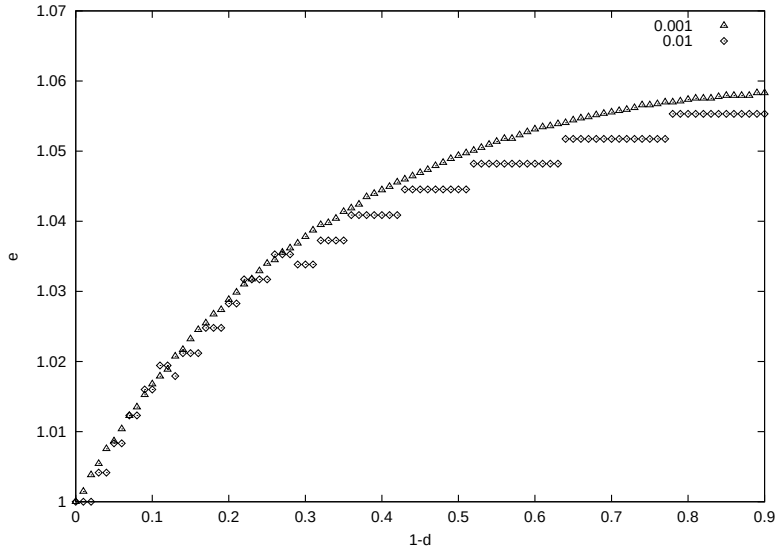

a) for a crack of one broken bond

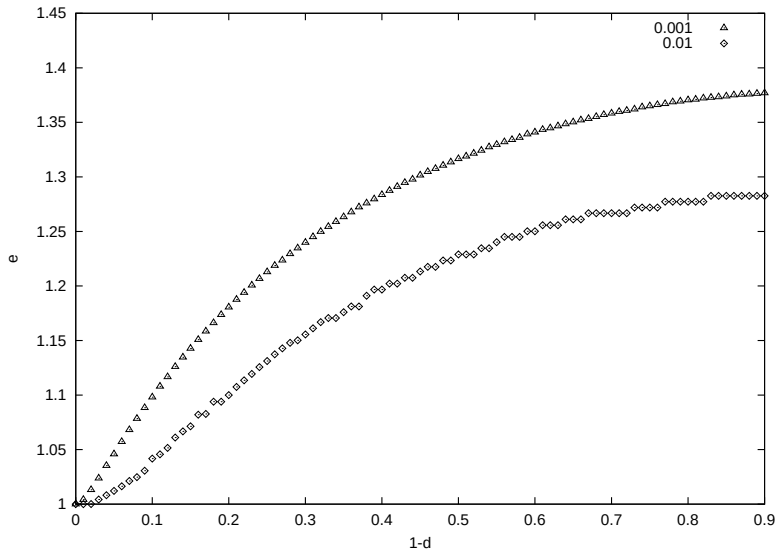

b) for a crack of ten broken bonds

Fig. 4.11: Bond length at the crack tip as a function of $1 - d$. $\epsilon = 0.001$, and $\epsilon = 0.01$ were considered. The lattice size $L = 50$ was used.

We see, in the 'higher disorder' ($\sigma = 0.06$) case early breakage reduces the energy in the system. Later on, the energy will not be released suddenly. The breakdown in energy corresponds to cracks which propagate due to their own dynamics (the relaxation can provide enough stress on the crack tip), and not due to decreasing d.
We see the dynamics of relaxation is highly relevant for the resulting crack pattern.

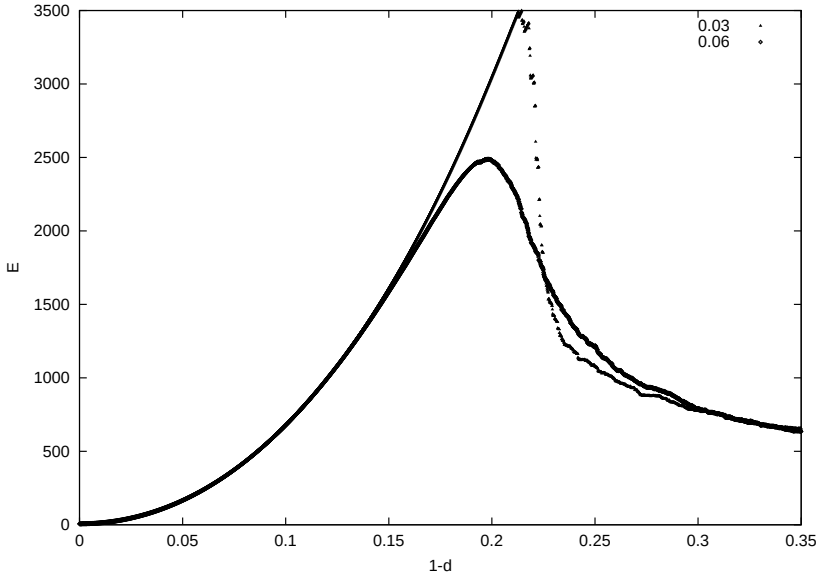

Fig. 4.12: The elastic energy as a function of $1 - d$ for $\sigma = 0.03$ (sharp peaked curve), and $\sigma = 0.06$. Here $L = 200$ and $\epsilon = 0.01$ were used. The figure just compares two single runs.

4.5 Characteristic length and slipping threshold

As pointed out in section 3.5 ϵ is inducing a characteristic length. We want to check if lengths in the pattern really scale like ϵ^{-1}. Calculations are performed with various ϵ, $L = 200$, $\sigma = 0.03$, and $d_{min} = 0.65$. Fig. 4.13 shows the typical results.

With increasing ϵ the pattern gets more disconnected, loops disappear. This phenomenon could be also observed in nature. Groisman et al. [7] studied the dependence of the pattern on the thickness of the layer. They found that in a sufficiently thin layer (of a coffee-water-mixture) many cracks do not join and no polygonal network was present.
As expected structures are bigger for smaller ϵ. To quantify this result the following techniques was used. The white area was filled with discs of uniform radius r, such that every disc had to be completely inside the white area. The total area of the union of all discs was calculated as a function of the their radius r. The result is a cumulative distribution of cell sizes r (here cells = islands and peninsulas). Assuming a Gaussian distribution of cell sizes (which seems to be the case) the characteristic cell size R was obtained as the value which halves the maximum (at $r = 0$) of the cumulative distribution. Linear interpolation was used to get non-integer values for R. Fig. 4.14 shows the dependence of the characteristic cell size R on ϵ. This analysis was performed on the pictures like in fig. 4.13 and not on the triangular lattice.
This technique proved to give much better (smaller error) results than from calculating correlation functions, which produce only slight heaps at $2R$. Problems can arise if small black pixels (which arise from tiny one-bond cracks) are inside big white cells (because than the white area does not cover the disc anymore). Therefore these pixels were removed by eroding the black areas. A boundary of diameter one pixel was removed. This erosion

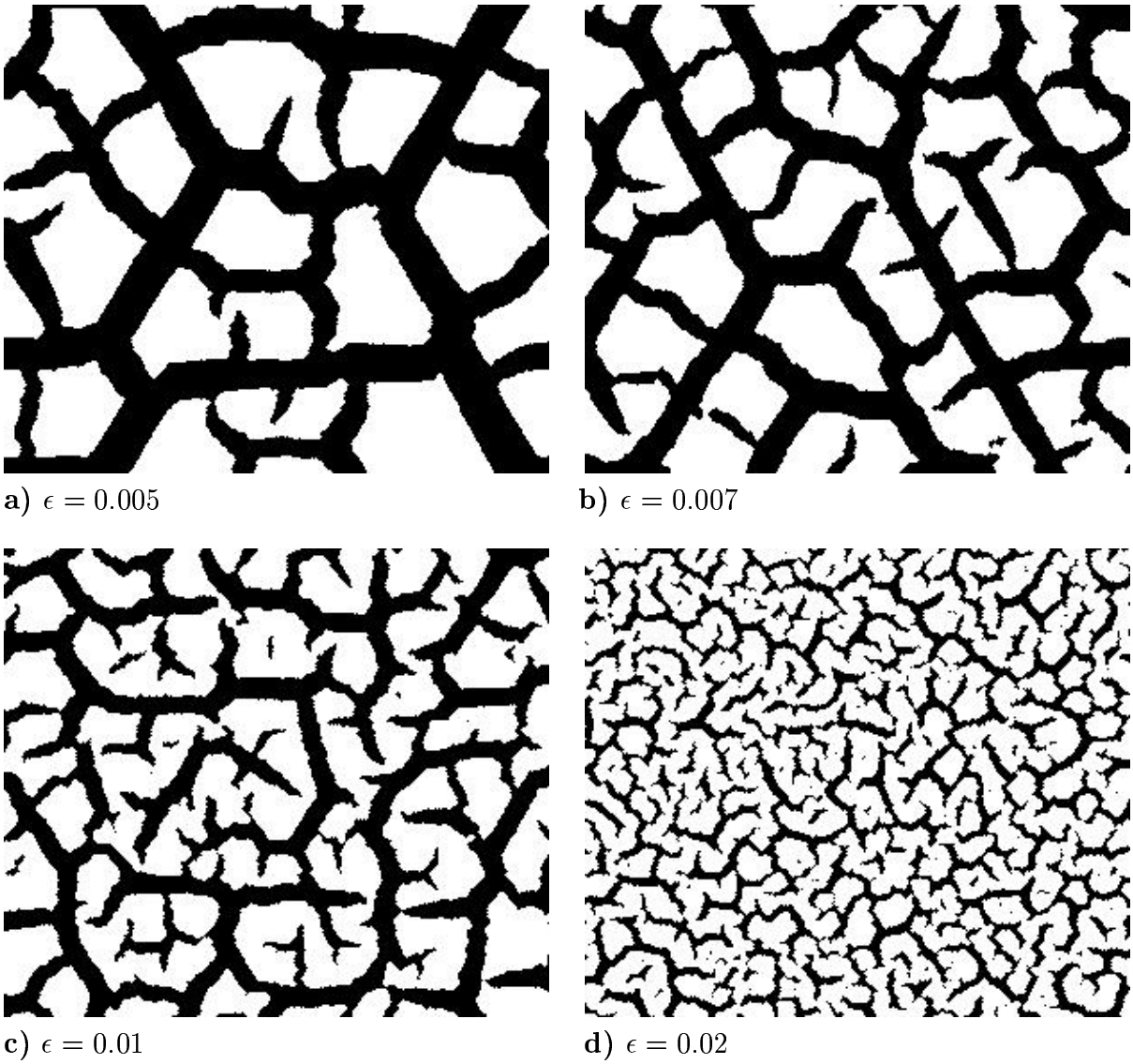

a) $\epsilon = 0.005$ **b)** $\epsilon = 0.007$

c) $\epsilon = 0.01$ **d)** $\epsilon = 0.02$

Fig. 4.13: The pictures show how ϵ alters the shape of a crack pattern. Lattice size $L = 200$ and $\sigma = 0.03$ were used.

was performed for all crack pattern pictures shown in this chapter.

As can be seen in fig. 4.14 the relation $R \propto \epsilon^{-1}$ is satisfied quite well, as predicted in section 3.5. The errors can be improved by using more pictures to analyze. Just one picture for $\epsilon = 0.02, 0.01, 0.007$, and two for $\epsilon = 0.005$ were used. The deviation for $\epsilon = 0.005$ is due to boundary effects (in this case bigger lattices should be used). A deviation for big ϵ ($\epsilon = 0.02$) can be expected (see fig. 3.7).

What happens if ϵ approaches 0. The torus will break catastrophically leaving just a single fragment with a boundary behind. Then this fragment will uniformly shrink with further decreasing d. No internal stresses will build up. This can be nicely illustrated with the one dimensional model using periodic boundary conditions. Think of a circle. As soon as one bond breaks, the remainder shrink together such that the length of every bond is d.

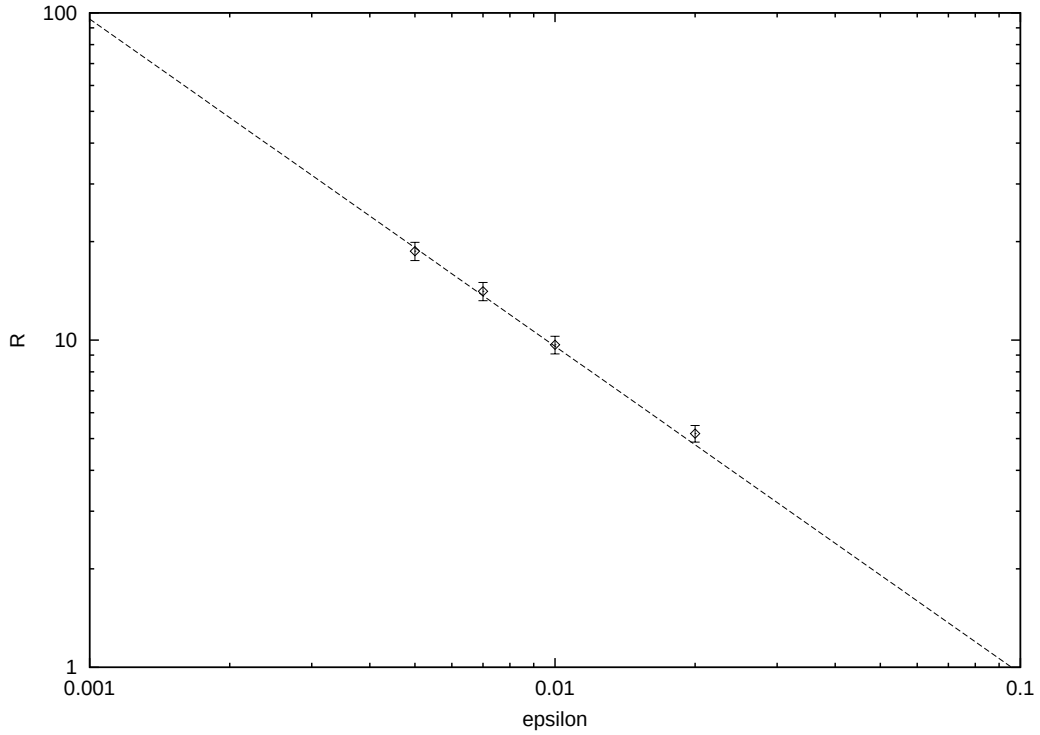

Fig. 4.14: The dependence of the characteristic cell size R on ϵ. A power-function with exponent -1 was fitted to the data. Error bars were estimated from the procedure of evaluating the size R.

4.6 Criticality

Is there something happening at σ_c (the transition point between patterns with loops and the ones without loops)? One might think that this transition could be attacked by means of renormalization theory. This would require scale-invariance at the transition point σ_c. It was investigated if the crack cluster sizes in the final crack pattern (at $d_{min} = 0.65$) loose a characteristic scale at σ_c. This was found not to be the case. Just looking at small lattice sizes ($L = 100$) seemed to allow power-laws. But, looking at bigger lattices ($L = 200$) did not confirm these power-laws. Above σ_c is the point where no percolation occurred. The lattice is still hold together by a robust net of springs. In the 'holes' of this net are the crack clusters. The cluster sizes of these cracks are distributed following approximately an exponential law. It is different in percolation theory [31], there, every single point belongs with the same probability p to a cluster. Approaching the critical value p_c for the existence of a percolating cluster from below (smaller p) the cluster sizes can be tuned arbitrarily close to being scale-invariant.
The characteristic length scale induced by ϵ in the model is of great importance. It seems to destroy every scale-invariance. We do not know exactly. A single crack can proceed much further than the characteristic length of the relaxation, driven by the high probability of breakage at the crack tip. Thus, it is not trivial. But, it seems likely that all the ideas about self-similarity are not useful to describe crack pattern.

Chapter 5

Experiments

An experiment was designed to observe a transition form a crack pattern percolating the system to a network of many not connected cracks. This was realized by choosing different proportions of sand and bentonite. The bentonite content is mainly responsible for the shrinkage of the material and provides thus a handle on that. Sand-water-mixtures will not develop any desiccation cracks, while a bentonite-water-mixture will break into many fragments.

5.1 Description of the experiment

Mixtures of sand (quartz sand), bentonite and water were prepared as a layer and let dry in fresh air at room temperature. Fig. 5.1 shows the setup.

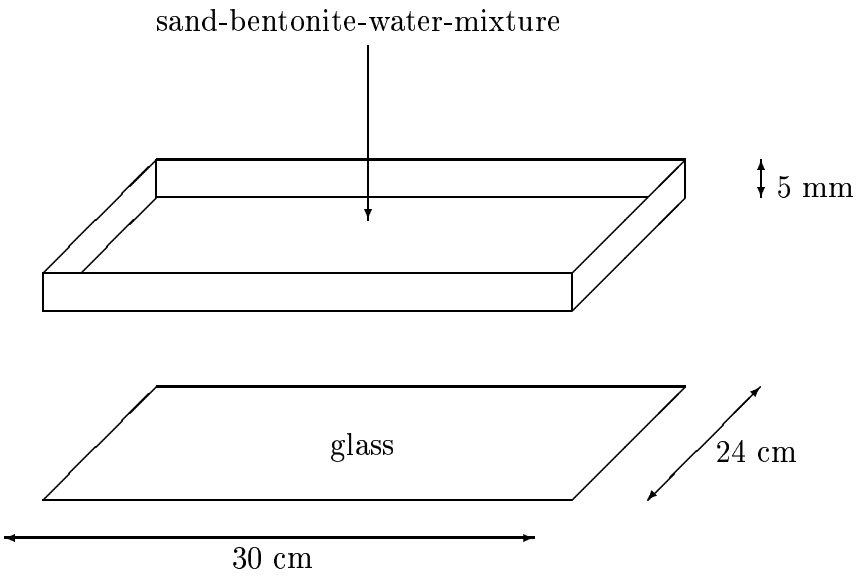

Fig. 5.1: Experimental setup. The mixture is put in between a metal frame on a glass plate.

Bentonite and sand were mixed before water was added. To get a layer of uniform thickness the mixture was flattened with a ruler to match the height of the metal frame, as shown in fig. 5.2.

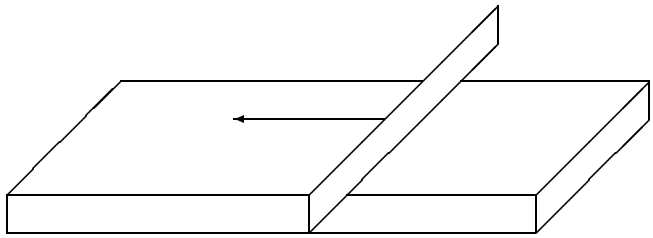

Fig. 5.2: The mixture was put in shape with a ruler.

The setup was put under a fume hood. It was protected from direct sunshine. At different stages of the desiccation process pictures were taken by a digital camera (with a resolution of $1520 * 1008$ pixels) and the the probe was weighed. To get a better contrast of the crack pattern the glass plate was put on a black sheet. Diffusive light proved to be the best. Lamps, focusing the setup, produced reflections on the glass plate. This caused severe problems to get binary images of the crack pattern. The initially colored pictures were transformed into grey scaled ones. A grey level threshold was used to get a binary image, with cracks colored black. This threshold was individually adapted, in a way that the digitalized crack pattern resembles best (by human judgement) the original one.
Throughout the experiments the temperature under the hood stayed about constant, $21.5 \pm 1°C$.

5.2 Results

5.2.1 The loop density

Initially, the mixture dominated by bentonite is very adhesive and gel like. In contrast the one with more sand is not adhesive and more fluid. Fig. 5.3 to 5.5 show the binary crack patterns for different sand:bentonite mixtures after the mixtures dried out completely (after about one and a half to two days). The pictures show a window size of $25.8{*}20.9\,cm^2$.

With decreasing bentonite content a transition from a polygonal network (with many crack loops and islands) to a system of disconnected cracks was observed. In between, islands transform to peninsulas (fig. 5.4b). This is very similar in the model (compare fig. 5.4b with fig. 4.5b). In fig. 5.5b the cracks seem to be oriented. This turned out to be an artifact. As seen in fig. 5.2, the mixture was flattened with a ruler. If the ruler was put on the probe in the perpendicular direction the cracks happened to be oriented also in the perpendicular direction.

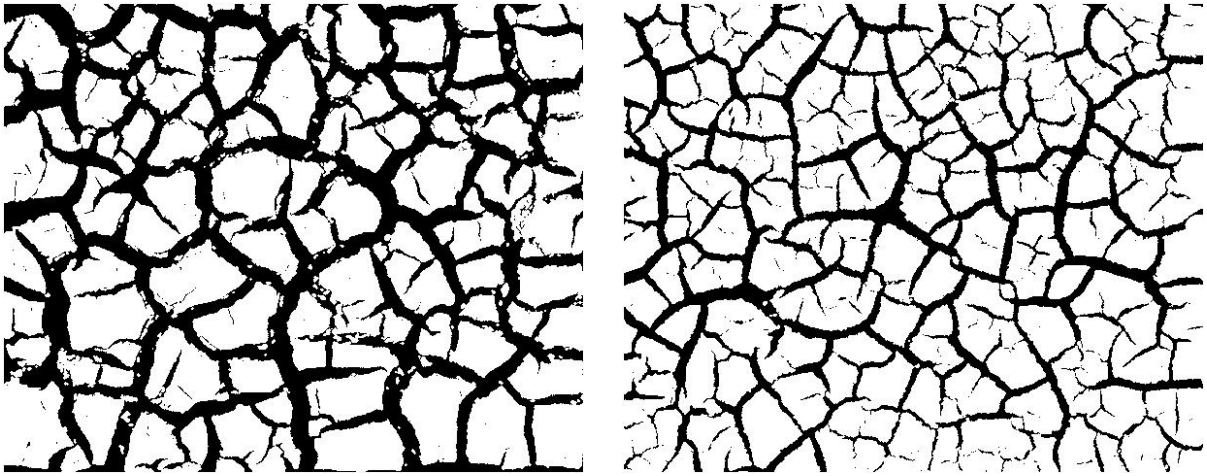

a) $m_s : m_b = 1 : 5$ **b)** $m_s : m_b = 1 : 1$

Fig. 5.3: The dependence of the crack pattern on the mass relation of sand to bentonite, after the probe dried out completely.

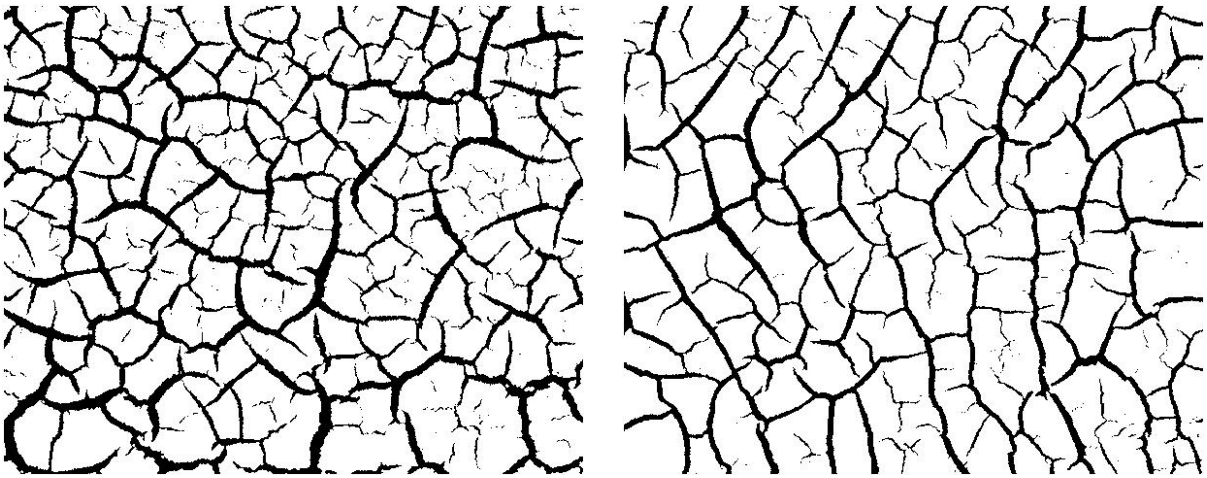

a) $m_s : m_b = 2 : 1$ **b)** $m_s : m_b = 4 : 1$

Fig. 5.4: The dependence of the crack pattern on the mass relation of sand to bentonite, after the probe dried out completely.

Table 5.1 shows the number of loops as obtained from the pictures in fig. 5.3 to 5.5. This is also illustrated in fig. 5.6. (Trivially, the number of loops depends on the size of the probe. Therefore, only the loop density (#loops/area) is of any physical meaning. Here, always the same area was considered.)
We see, that looking at a crack pattern and counting loops provides an interesting tool to say something about the local composition of the material. But, it has to be considered that the thickness of the layer and the strength of the binding to a substrate influences the loop density.

Fig. 5.6 shows a similar result as obtained from the model (see fig. 4.6 to 4.8). The high

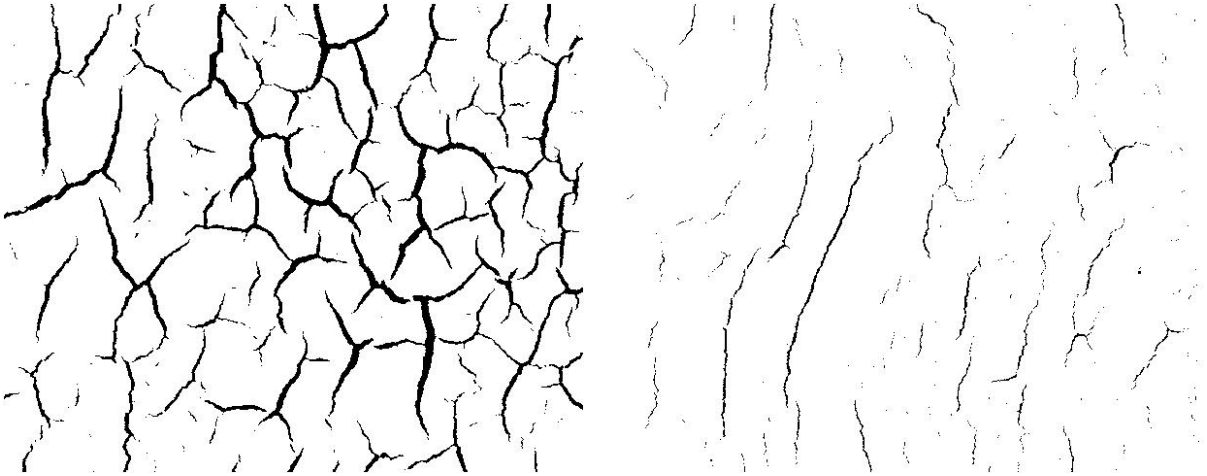

a) $m_s : m_b = 5 : 1$ **b)** $m_s : m_b = 10 : 1$

Fig. 5.5: The dependence of the crack pattern on the mass relation of sand to bentonite, after the probe dried out completely.

$m_s : m_b$	#loops
1:5	173
1:1	63
2:1	46
4:1	15
5:1	0
10:1	0

Table 5.1: The dependence of the number of loops in the crack pattern on the sand to bentonite mass relation ($m_s : m_b$).

loop number for $m_s : m_b = 0.2$ is understandable with a look at fig. 5.3a. Many small fragments lie in between the cracks. Any isolated fragment will be counted as a loop.
Now, there seems to be a connection between $m_s : m_b$ and σ. The main difference between clay and sand is the mean grain size (sand grains are much bigger). We propose that a mixture of different grain sizes provides a handle on the disorder in the distribution of cracking thresholds. Comparing the dynamics of the crack pattern for the probes in fig. 5.3a and fig. 5.5a it could be observed that cracks appear sooner in the case with more sand (after about 2h vs. 5h). This is similar to the dynamics for low and high disorder. But, also of big importance is the water content in the initially prepared probe (see table 5.2). Bentonite can store more water, and will therefore contract further. This results in a broader relaxation range as obtained for smaller ϵ in the model. Thus, $m_s : m_b$ probably influences σ as well as ϵ.

The difference to the dependence on σ is that crack densities in the layers with high sand content are not as high as in the model for large σ (compare fig. 5.5b with fig. 4.5d). The reason is that we contracted the relaxed spring length d for all σ to the same value. While in the sandy case the water content is lower. Thus, it cannot contract as far.

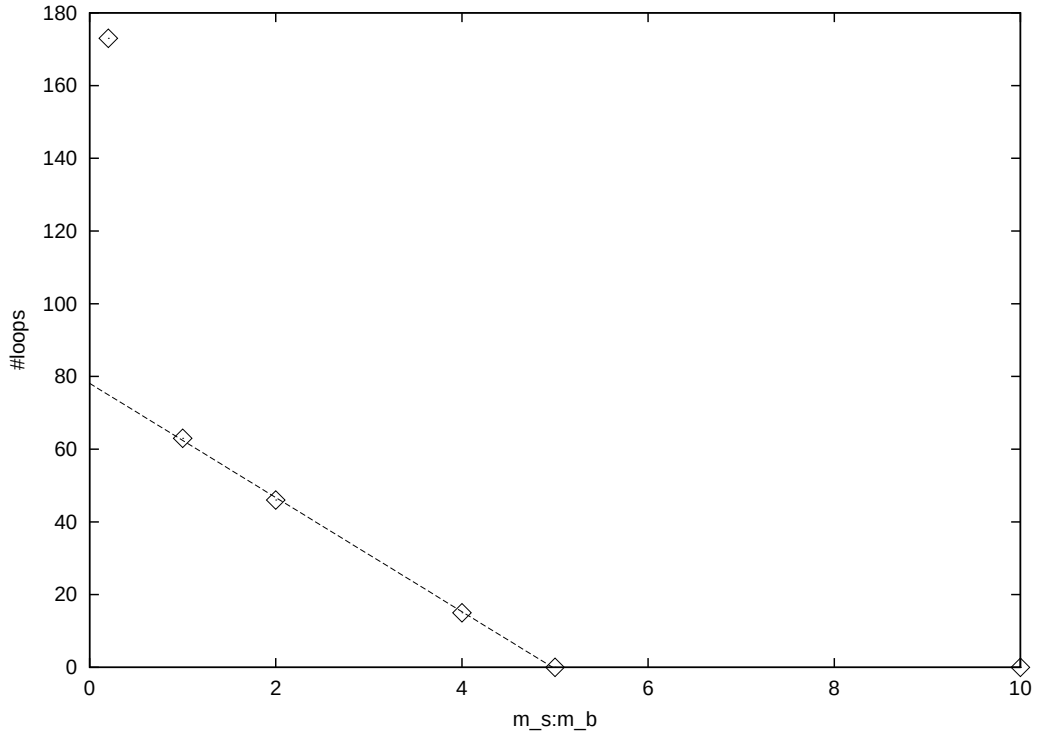

Fig. 5.6: The dependence of the number of loops in the crack pattern on the sand to bentonite mass relation ($m_s : m_b$).

$m_s : m_b$	1:5	1:1	2:1	4:1	5:1	10:1
θ	0.620	0.589	0.531	0.408	0.364	0.316

Table 5.2: Relative mass content θ of water in the probe.

Like in the model (section 4.6) the crack cluster sizes (area) at the point where the loops vanish ($m_s : m_b = 5$) were found not to be scale-invariant. But, we just investigated the cracks in fig. 5.5a. Thus, the data is very weak.

5.2.2 Pattern dynamics

As in the model (see fig. 4.3) cracks popped into sight as single not connected structures. The merging into loops happened at later stages. Cracks formed independently rather than on the boundary of existing cracks. Not enough pictures were taken during the desiccation process to investigate if loops occur at the same time as percolation (see section 4.2).

In fig. 5.7a, the pattern on the lower part of the picture differs from the one on the upper part. The reason is that the layer dried out sooner on the lower part. Airflow under the fume hood probably caused this non-uniform conditions.

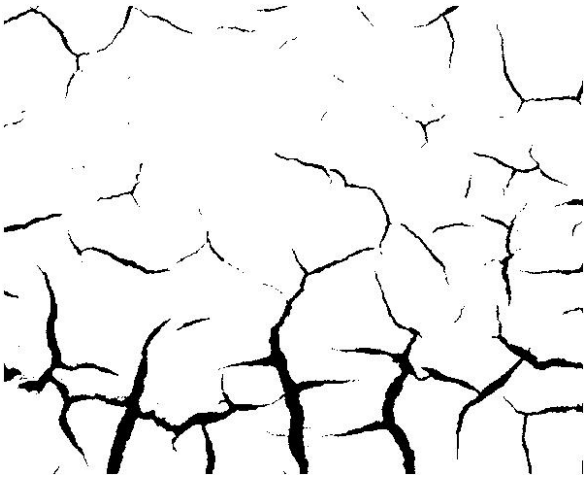

a) after 12.2h

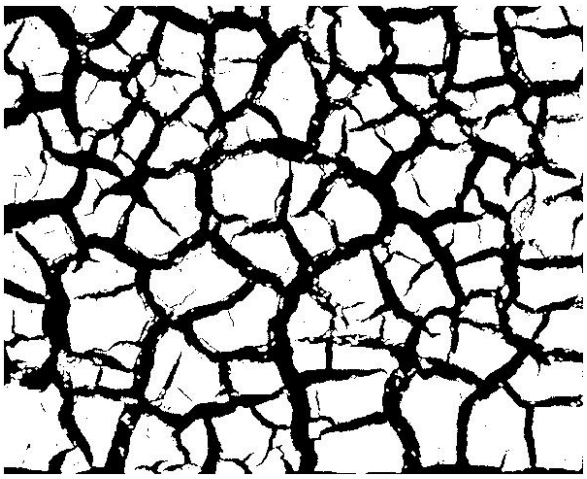

b) dried (after 2 days)

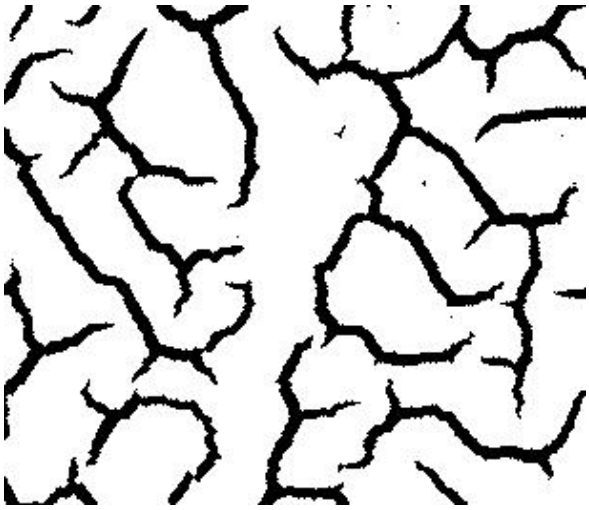

c) at $d = 0.769$

d) at $d = 0.664$

Fig. 5.7: The evolution of the crack pattern. In a and b the bentonite-sand mixture for $m_s : m_b$=1:5 compared with the pictures taken from the model in c and d (same as in fig. 4.3).

Chapter 6

Conclusions

- Our numerical model was able to produce crack patterns which resemble those found in nature.
- It was found that the appearance of percolation and loops happened to be at the same desiccation time. I encourage experiments to figure out if this is a real phenomena occurring in nature. It is very crucial for these experiments to obey uniform desiccation.
- Varying the parameter σ (standard deviation of the stress threshold) a transition could be observed from a pattern consisting of convex islands to one consisting of disconnected cracks. A similar transition could be found by varying the parameter ϵ (slipping threshold) or the bentonite-sand mass relation in the experiment. The results suggest that the ability of the material to relax (relaxation range) plays an important role in the observed transition. More theoretical work need to be done in this direction.
- Counting loops in the topology of the crack pattern proved to be a possibility to quantify the transition. Therefore, the loop number deals as an order parameter (whose value vanishes on one side of the transition).
- The presented work gives some insight on the impact of friction on the crack pattern. Friction induces a characteristic scale in the pattern. We suggest therefore that the idea of self-similarity is the wrong way to describe desiccation patterns.

Appendix A

Implementation of the relaxation in C

A.1 Optimizations

- A single loop is used for the whole lattice.
- Calculation at a node is omitted if nothing at its neighborhood bonds happened the previous time step. This is realized with a newly developed two-color system.

These optimizations do not claim to be optimal.

A.1.1 The two-color system

Every node can have two colors, called red and blue. It is possible that a node has all two colors or is not colored at all. Calculation is only done on the red nodes. After the calculation was performed the red color is removed. If the node was moved all its neighbors (which are connected to the node via a bond) are colored blue. After this is done for all nodes (now no single node is red) every blue color is turned into red. Additionally, if one bond is removed the two nodes connected to this bond are color red, and in the beginning and every time after the value d (relaxed spring length) is changed all nodes are colored red.
The idea is that if nothing happens at the nodes in the neighborhood it is not necessary to calculate a new equilibrium position, nothing new can happen.

A.2 Newton-Raphson relaxation for node i

int pointrelax(modelparam param,long i,float *olddux,float *oldduy,int repeat)
{
First start of precedure during the relaxation iteration for node i: repeat = 0
else: repeat = 1

```
param.d: relaxed spring length
param.bitfeld[i]: stores the colors and information about broken bonds,
bit 1-3: the three bonds at node i: value=0: bond is removed, else value=1
bit 4: value=1: red, else not-red
bit 5: value=1: blue, else not-blue

float fx,fy; first derivative of the energy as a function of the position of node i
float fxx,fxy,fyy; Hesse-matrix of the energy, fyx=fxy
float detH,invdetH; determinant of the Hesse-matrix and its inverse
float dx,dy,sqrdx,sqrdy,sqrd,dux,duy;
double sqrdist,dist;
int nb,moved=0,bond,verb;
long ni,vi;
long n_2;

sqrd = param.d*param.d;
n_2 = param.n/2;

fx = fy = 0;
fxx = fyy = fxy = 0;

sum over the 6 neighbors of i
calculate the first two derivatives of the energy:

for(nb=1;nb<=6;nb++)
{
   ni = neighbor(nb,i,param.n,param.sqrn); neighbor number nb of i (incl. p.b.c.)
   verb = (nb-1)%3 + 1;
   if (nb<=3) vi = i; else vi = ni;
   bond = (1<<verb-1 & param.bitfeld[vi]) >> verb-1;

   if (bond) if the bond is not broken
   {
      dx = param.neux[i]-param.ux[ni];
      dy = param.neuy[i]-param.uy[ni];

      take care of the periodic boundary conditions (p.b.c.):
      if (dx> n_2) dx -= param.n;
      if (dx< -n_2) dx += param.n;
      if (dy> n_2) dy -= param.n*SQRT3div2;
      if (dy< -n_2) dy += param.n*SQRT3div2;

      sqrdx = dx*dx;
      sqrdy = dy*dy;
```

```
      fx += dx*(sqrdx+sqrdy-sqrd);
      fy += dy*(sqrdx+sqrdy-sqrd);

      fxx += 3*sqrdx+sqrdy-sqrd;
      fxy += 2*dx*dy;
      fyy += 3*sqrdy+sqrdx-sqrd;
   }
}


Newton-Raphson:
detH = fxx*fyy-fxy*fxy;
invdetH = 1/detH;

change in the coordinates of node i:
dux = (fx*fyy-fy*fxy)*invdetH;
duy = (-fx*fxy+fy*fxx)*invdetH;

sqrdist = (double)(dux)*dux+(double)(duy)*duy;

if (sqrdist>=SQREPSILON)
{
   param.neux[i] = param.neux[i] - dux;
   param.neuy[i] = param.neuy[i] - duy;
   moved=1;
   if the new step (dux,duy) points in the opposite direction than the previous step
   the iteration is stopped to avoid endless oscillations:
   if (repeat && (*olddux)*dux+(*oldduy)*duy<0) moved=0;
}
return moved;
}
```

A.3 Relaxation of the whole lattice

```
int relax(modelparam param)
{
lattice size: n*n
coordinates of the nodes: param.ux, param.uy
temporary coordinates: param.neux, param.neuy

long i,ni,vi;
int moved,nb,verb,bond;
int noSilence=0; if any node moves noSilence is set to 1
float olddux,oldduy;
```

```
relax the whole lattice one step:

for(i=1;i<=param.sqrn;i++)
{
   param.neux[i]=param.ux[i];
   param.neuy[i]=param.uy[i];
   if ((8 & param.bitfeld[i]) >> 3 == 1) if the node is red
   {
      moved=pointrelax(param,i,&altdux,&altduy,0);
      if (moved)
      {
         noSilence=1;

         paint neighbors blue (bit5=1):
         for(nb=1;nb<=6;nb++)
         {
            ni = neighbor(nb,i,param.n,param.sqrn); neighbor number nb of i
            verb = (nb-1)%3 + 1;
            if (nb¡=3) vi = i; else vi = ni;
            bond = (1<<verb-1 & param.bitfeld[vi]) >> verb-1;
            if (bond) param.bitfeld[ni] = param.bitfeld[ni] | 16;
         }
         while (moved) moved=pointrelax(param,i,&olddux,&oldduy,1);
      }
      remove the red color if there was no change in position:
      else param.bitfeld[i] = param.bitfeld[i] & 23; 0001 0111
   }
}

renew all coordinates:
for (i=1;i<=param.sqrn;i++)
{
   if ((8 & param.bitfeld[i]) >> 3 == 1) if the node is red
   {
      param.ux[i]=(param.neux[i]-param.ux[i])*LAMBDA+param.ux[i];
      param.uy[i]=(param.neuy[i]-param.uy[i])*LAMBDA+param.uy[i];
      remove the red color:
      param.bitfeld[i] = param.bitfeld[i] & 23;
   }
   if blue, color red and remove blue:
   if ((16 & param.bitfeld[i]) >> 4 == 1)
      param.bitfeld[i]=(param.bitfeld[i] | 8) & 15; 0000 1111
}
return noSilence;
}
```

Bibliography

[1] J. Åström, M. Alava, and J. Timonen. Crack dynamics and crack surfaces in elastic beam lattices. *Phys. Rev. E*, 57:1259–1262, 1998.

[2] M.F. Barnsley. *Fraktale*. Spektrum Akademischer Verlag, Heidelberg, 1995.

[3] J.J. Binney, N.J. Dowrick, A.J. Fisher, and M.E.J. Newman. *The theory of critical phenomena*. Oxford University Press, Oxford, 1993.

[4] H. Colina, L. de Arcangelis, and S. Roux. Model for surface cracking. *Phys. Rev. B*, 48:3666–3676, 1993.

[5] J. Fineberg, S.P. Gross, M. Marder, and H.L. Swinney. Instability in the propagation of fast cracks. *Phys. Rev. B*, 45:5146–5154, 1992.

[6] T. Gramss, editor. *Non-standard computation*. Wiley-VCH, Weinheim, 1998.

[7] A. Groisman and E. Kaplan. An experimental study of cracking induced by desiccation. *Europhys. Lett.*, 25:415–420, 1994.

[8] D. Hallett, A.R. Dexter, and J.P.K. Seville. The application of fracture mechanics to crack propagation in dry soil. *Europ. J. Soil Sci.*, 46:591–599, 1995.

[9] A. Hansen, S. Roux, and H.J. Herrmann. Rupture of central-force lattices. *J. Phys. France*, 50:733–744, 1989.

[10] Y. Hayakawa. Pattern selection of multicrack propagation in quenched crystals. *Phys. Rev. E*, 50:1748–1751, 1994.

[11] P. Heino and K. Kaski. Mesoscopic model of crack branching. *Phys. Rev. B*, 54:6150–6154, 1996.

[12] K. Hirota, Y. Tanoue, and T. Kaneko. Generation of crack patterns with a physical model. *The Visual Computer*, 14:126–137, 1998.

[13] G.W. Horgan and I.M. Young. An empirical stochastic model for the geometry of two-dimensional crack growth in soil. *Geoderma*, 96:263–276, 2000.

[14] T. Hornig, I.M. Sokolov, and A. Blumen. Patterns and scaling in surface fragmentation processes. *Phys. Rev. E*, 54:4293–4298, 1996.

[15] H.J. Jensen. *Self-Organized Criticality.* Cambridge University Press, Cambridge, 1998.

[16] S. Kitsunezaki. Fracture patterns induced by desiccation in a thin layer. *Phys. Rev. E*, 60:6449–6464, 1999.

[17] W. Korneta, S.K. Mendiratta, and J. Menteiro. Topological and geometrical properties of crack patterns produced by thermal shock in ceramics. *Phys. Rev. E*, 57:3142–3152, 1998.

[18] A.R. Leach. *Molecular modelling.* Addison Wesly Longman, Essex, 1996.

[19] K.-T. Leung and J.V. Andersen. Phase transition in a spring-block model of surface fracture. *Europhys. Lett.*, 38:589–594, 1997.

[20] A. Malthe-Sørenssen, T. Walmann, J. Feder, T. Jøssang, P. Meakin, and H. H. Hardy. Simulation of extensional clay fractures. *Phys. Rev. E*, 58:5548–5564, 1998.

[21] A. Malthe-Sørenssen, T. Walmann, B. Jantveit, J. Feder, and T. Jøssang. Simulation and characterization of fracture patterns in glaciers. *J. Geophys. Res.*, 104:23,157–23,174, 1999.

[22] M. Marder and J. Fineberg. How things break. *Physics Today*, pages 24–29, 9 1996.

[23] P. Meakin. A simple model for elastic fracture in thin films. *Thin Solid Films*, 15:165–190, 1987.

[24] Z. Olami, H.J.S. Feder, and K. Christensen. Self-organized criticality in a continuous, nonconservative cellular automaton modeling earthquakes. *Phys. Rev. Lett.*, 68:1244–1247, 1992.

[25] W.H. Press. *Numerical recipes in C.* Cambridge University Press, Cambridge, 1992.

[26] C.H. Scholz. *The mechanics of earthquakes and faulting.* Cambridge University Press, Cambridge, 1990. section 1.1.

[27] E. Sharon and J. Fineberg. Microbranching instability and the dynamic fracture of brittle materials. *Phys. Rev. B*, 54:7128–7139, 1996.

[28] E. Sharon, S.P. Gross, and J. Fineberg. Local crack branching as a mechanism for instability in dynamic fracture. *Phys. Rev. Lett.*, 74:5096–5099, 1995.

[29] K.A. Shorlin, J.R. de Bruyn, M. Graham, and S.W. Morris. Development and geometry of isotropic and directional shrinkage-crack patterns. *Phys. Rev. E*, 61:6950–6957, 2000.

[30] A.T. Skjeltorp and P. Meakin. Fracture in microsphere monolayers studied by experiment and computer simulation. *Nature*, 335:424–426, 1988.

[31] D. Stauffer and A. Aharony. *Introduction to percolation theory.* Taylor and Francis Group, London, 1992.

[32] J. Walker. Cracks in a surface look intricately random but actually develop rather systematically. *Sci. Am.*, 255:178–183, 10 1986.